

Post Processing Covid-19 Forecasts

Matthias Herp, Joel Beck

supervised by

Nikos Bosse

Chair of Statistics, University of Göttingen

15.03.2022

Table of Contents

1	Introduction	2
2	Analysis Tools	2
2.1	Data & Methodology	2
2.2	The <code>postforecasts</code> Package	5
3	Conformalized Quantile Regression	8
3.1	Traditional CQR	8
3.2	Asymmetric CQR	14
3.3	Multiplicative CQR	18
4	Quantile Spread Adjustment	22
4.1	Theory	22
4.2	Optimization	23
4.3	Results	25
5	Method Comparison	32
5.1	Ensemble Model	32
5.2	Comparison of CQR, QSA & Ensemble	34
6	Conclusion	38
A	QSA Appendix	40
	References	41

1 Introduction

Forecasts can play an important role in informing public policy and personal decision making. During the Covid-19 pandemic, for example, governments and public support for political action, relied heavily on predictions of future case and death numbers. As epidemic developments depend on numerous factors including the decision processes of individuals, there is inherent uncertainty in epidemic forecasts. Thus, there is a growing consensus that these infectious disease forecasts should be probabilistic in nature (Bracher et al. 2021).

Many forecasts, however, tend to be overconfident: A comprehensive review found that observed values were within the 95% confidence intervals for only 75% of predictions (Gnanvi et al. 2021). One approach to improve forecasts in terms of their confidence interval coverage, is *post-processing*. The idea is to adjust forecast uncertainty in form of prediction quantiles systematically, e.g. by a fixed value or a certain factor based on the percentage of observations which were covered by the prediction intervals in the past.

We apply post processing methods to human forecasts from the *UK Covid-19 Crowd Forecasting Challenge* (EpiForecasts 2021b) as well as model based forecasts provided by the *European Covid-19 Forecast Hub* (EpiForecasts 2021a). Using these data sets we examine the contributions post-processing techniques can provide and their effects among varying *models*, *target types* (i.e. Covid-19 Cases or Deaths), forecast *horizons* and *quantiles*.

In order to provide a well-organized infrastructure for our analysis, simplify further extensions and provide a basis which other researchers can use to investigate post-processing methods, we developed the **postforecasts** R package. This report introduces the package, its use and provides examples through our analysis of the Covid-19 forecasts.

The report is divided into the following sections: Section 2 introduces the two data sets and the main functions of the **postforecasts** package. Section 3 presents post-processing methods based on *Conformalized Quantile Regression*, including a theoretical introduction as well as an analysis of their performance on the data. Section 4 builds on top of this structure by introducing *Quantile Spread Adjustment* based post-processing methods and explores their results. Section 5 compares all implemented methods and proposes an ensemble model. Finally, Section 6 summarizes the results and discusses their implications.

2 Analysis Tools

Data Analysis is inherently build upon two fundamental components: High Quality Data that allows to gain insight into the underlying data generating process and a structured and reproducible way to extract information out of the collected data.

Section 2.1 introduces the two data sets we worked with whereas Section 2.2 provides an overview about the **postforecasts** package, a unified framework to apply and analyze various post-processing techniques.

2.1 Data & Methodology

This section first describes the two data sources that all of our analysis is based on. The final paragraphs explain our evaluation procedure from a theoretical point of view.

2.1.1 UK Covid-19 Crowd Forecasting Challenge

As part of an ongoing research project by the EpiForecasts¹ group at the London School of Hygiene & Tropical Medicine, the *UK Covid-19 Crowd Forecasting Challenge* (EpiForecasts 2021b) consisted of submitting weekly predictions of Covid-19 Cases and Deaths in the United Kingdom in 2021. The challenge was not restricted to experienced researchers in the field but rather intended to collect quantile predictions for the upcoming four weeks by non-expert individuals.

¹<https://epiforecasts.io/>

One of the main motivations was to gather evidence for or against the hypothesis that humans are highly capable of precise *point forecasts*. Yet, at the same time, they tend to be too confident in their beliefs such that prediction *intervals* are chosen too narrow. In fact, this tendency presents one motivation for post-processing: Extract valuable information from point forecasts and adjust the corresponding prediction intervals with a systematic correction procedure.

In case of individuals that are unfamiliar with statistical methodology, specifying forecasts for very specific quantiles of the predictive distribution might lead to inconsistencies. Therefore all participants could determine an uncertainty parameter around their median prediction via an interactive web application such that all quantile predictions could be concluded in an automatic fashion. Note that this procedure inherently leads to *symmetric* forecast intervals. The results of the 12-week challenge are publicly available².

2.1.2 European Covid-19 Forecast Hub

According to their webpage the *European Covid-19 Forecast Hub* (EpiForecasts 2021a) collects “short-term forecasts of Covid-19 cases and deaths across Europe, created by a multitude of infectious disease modelling teams”.

In contrast to the compact UK data described above, the European Forecast Hub data contains almost two million observations for over 20 European countries. Further, the forecasters are knowledgeable research groups that submit their weekly predictions based on statistical models. Although the data collection continues in regular frequency up to this day, our data set is limited to a 32-week span from March 2021 until October 2021.

The overall structure of the two data sets introduced above is very similar. Since we will refer to some particularly important columns by name frequently throughout the next chapters, they are briefly described here:

- **location:** The country for which the forecasts were submitted. Equals **GB** for the UK data. Our analysis for the European Forecast Hub data selects 18 different European countries.
- **model:** The forecaster (group). Mostly (non-expert) individuals for the UK data and international research groups for the European Forecast Hub.
- **target_type:** Either Covid-19 Cases or Covid-19 Deaths.
- **horizon:** The time horizon how far in advance the predictions were submitted. Ranges from 1 week-ahead to 4 weeks-ahead.
- **forecast_date:** The exact date when the forecasts were submitted.
- **target_end_date:** The exact date for which the forecasts were submitted.
- **quantile:** One of 23 different quantile values ranging from 0.01 to 0.99.
- **prediction:** The predicted value for one specific combination of the variables above.
- **true_value:** The actual, observed number of Covid-19 Cases or Deaths. This value is repeated 23 times, once for each quantile value.

2.1.3 Weighted Interval Score

In order to quantify if the post-processed prediction intervals improve the original forecasts we chose the *Weighted Interval Score* (WIS) (Bracher et al. 2021) as our evaluation metric. The WIS is a so-called *Proper Scoring Rule* (Gneiting and Raftery 2007): It incentivizes the forecaster to state their true best belief and cannot be manipulated in favour of own interests. It combines measures for interval *sharpness* as well as *overprediction* and *underprediction* and can thus be understood as a trade-off between interval *coverage* and *precision*.

²<https://epiforecasts.io/uk-challenge/>

More specifically, for a given quantile level α , true observed value y as well as lower bound l and upper bound u of the corresponding $(1 - \alpha) \cdot 100\%$ prediction interval, the *Interval Score* according to Bracher et al. (2021) is computed as

$$IS_\alpha(y) = (u - l) + \frac{2}{\alpha} \cdot (l - y) \cdot \mathbb{1}(y \leq l) + \frac{2}{\alpha} \cdot (y - u) \cdot \mathbb{1}(y \geq u).$$

The penalties $\frac{2}{\alpha} \cdot (l - y)$ and $\frac{2}{\alpha} \cdot (y - u)$ for over- and underprediction are thus influenced by two components:

- The penalty gets larger for increasing distance of the true value y to the lower or upper bound, given that y is not contained in the interval.
- The penalty gets larger for smaller values of α , i.e. for higher nominal coverage levels $(1 - \alpha)$.

A set of K Interval Scores with different quantile levels $\alpha_1, \dots, \alpha_K$ can be aggregated to a single number, the *Weighted Interval Score*, via the formula

$$WIS(y) = \frac{1}{K + 0.5} \cdot (w_0 \cdot |y - m| + \sum_{k=1}^K w_k \cdot IS_{\alpha_k}(y)),$$

where m represents the predicted median.

Thus, as the name suggests, the Weighted Interval Score is a weighted sum of the individual Interval Scores. The weights w_k are typically chosen as $w_k = \frac{\alpha_k}{2}$ and the weight w_0 for the deviation of the median is usually set to 0.5.

2.1.4 Time Series Cross Validation

Just like any statistical model the post-processing methods must be evaluated on *out-of-sample* data. Rather than starting from the raw data, i.e. the observed Covid-19 Cases and Deaths, our data sets already consist of existing quantile predictions. As a consequence, no part of our data set must be dedicated to fitting the quantile regression models in the first place.

Our evaluation procedure can be split into two steps:

1. Use a *training set* to learn parameters of the post-processing procedure in consideration.
2. Use a *validation set* to evaluate how the learned parameters generalize to unseen data.

Instead of a hard cut-off between the splits we used *Time Series Cross Validation* to leverage a higher fraction of the data set for training. In contrast to classical Cross Validation for independent and identically distributed data, Time Series Cross Validation iterates through the data set along the time dimension one step at a time.

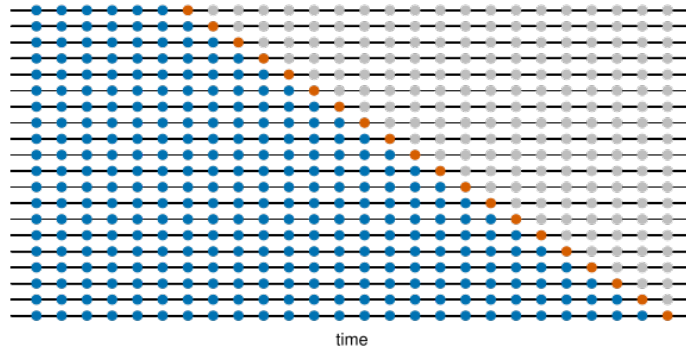


Figure 1: Time Series Cross Validation

The process is nicely illustrated in Figure 1³. At each iteration the validation set is composed of the one step ahead prediction based on all observations prior to and including the current time point. The algorithm

³Image Source: <https://otexts.com/fpp3/tscv.html> (Hyndman and Athanasopoulos 2021).

typically starts with a minimum number of observations as the initial training set, which can be considered a hyperparameter that has to be specified at the beginning of training.

2.2 The `postforecasts` Package

One core aspect of our project was the development of a fully functional package in the statistical programming language `R` (R Core Team 2021) that unites a collection of different post-processing algorithms into a well-designed and user friendly interface. This section can be understood as a compact guide how to use our package effectively and explains parts of the thought process that went into the implementation. It is worth noting that the `postforecasts` package adheres to all formal requirements for an `R` package and can be installed from our GitHub⁴ repository, where the source code is publicly available.

2.2.1 Overview

The `postforecasts` functions exported to the end-user can be grouped into three categories:

1. Exploratory

The `plot_quantiles()`, `plot_intervals()` and `plot_intervals_grid()` functions visualize the development of true Covid-19 Cases and Deaths over time as well as corresponding original and adjusted quantile predictions.

2. Model Fitting

The `update_predictions()` function is the workhorse of the entire `postforecasts` package. It specifies both the raw data and the post-processing method(s) that should be applied to the data set. The function returns a list of $k + 1$ equally shaped data frames for k selected post-processing methods where the first element is given by the original, possibly filtered, data frame.

All list elements can be analyzed separately or collectively by stacking them into one large data frame with the `collect_predictions()` function. The combined data frame is designed to work well with analysis functions of the `scoringutils`⁵ package (Bosse, Sam Abbott, and Gruson 2022). If multiple post-processing methods are applied, an ensemble model of all selected methods can be added via the `add_ensemble()` function, which lets the user access both the weighted ensemble predictions and a data frame with the corresponding weights.

3. Evaluation

As noted in Section 2.1 the Weighted Interval Score is our primary metric to evaluate the *quality* of prediction intervals. The `score()` function of the `scoringutils` package computes this quantity for each observation in the data set which can then be aggregated by the related `summarise_scores()` function.

Depending on the *granularity* of the aggregation the output might contain many interval scores of vastly different magnitudes. To simplify interpretation the `eval_methods()` function computes *relative* or *percentage* changes in the Weighted Interval Score for each selected method compared to the original quantile predictions. Further, these relative changes can be visualized by the `plot_eval()` function.

The following section demonstrates the complete workflow described above to give an impression of the *interaction* between the functions.

2.2.2 Workflow

We use the Covid-19 data for Germany in 2021 that is provided by the European Forecast Hub.

Figure 2 illustrates the 5%, 20% 80% and 95% quantile predictions of the `EuroCOVIDhub-ensemble` forecasting model during the summer months of 2021 in Germany.

⁴<https://github.com/nikosbosse/post-processing-forecasts>

⁵<https://epiforecasts.io/scoringutils/>

```
plot_quantiles(
  hub_germany,
  model = "EuroCOVIDhub-ensemble", quantiles = c(0.05, 0.2, 0.8, 0.95)
)
```

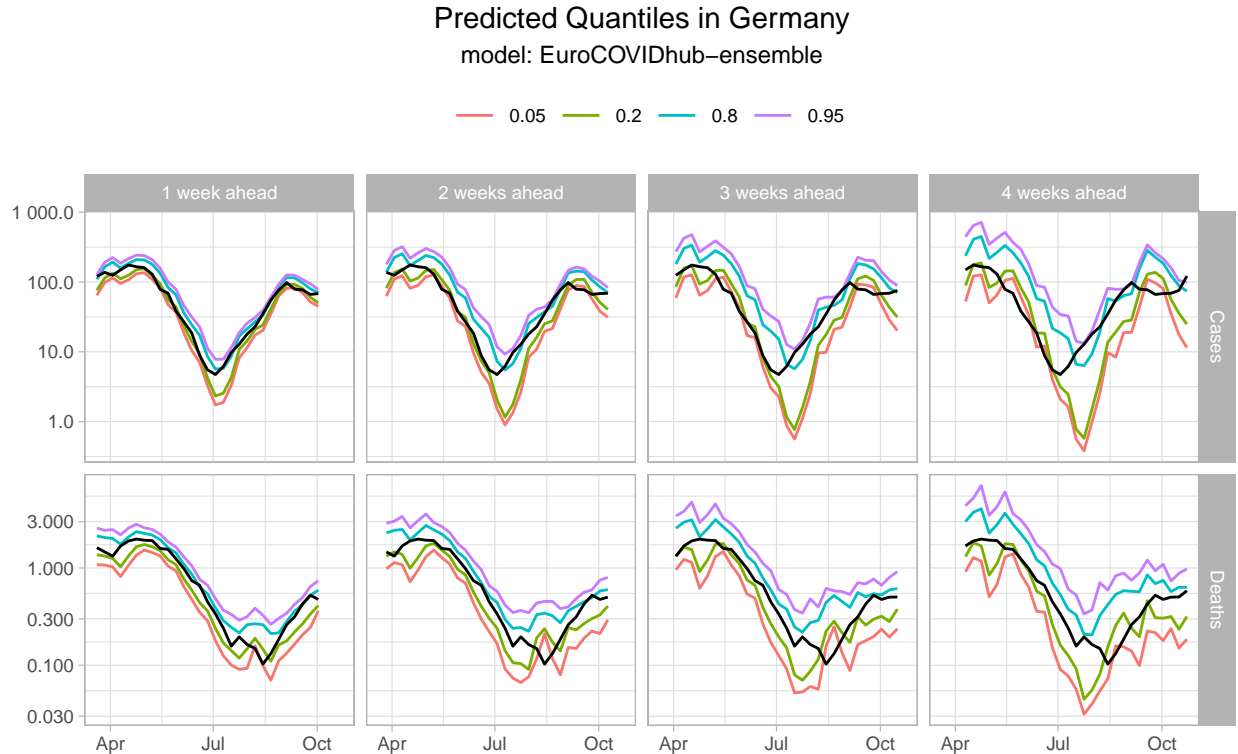


Figure 2: Original Quantile Predictions for Covid-19 Cases and Deaths in Germany 2021

The original predictions look quite noisy overall with the clear trend that uncertainty and, hence, the interval width increases with growing forecast horizons. We want to analyze if one particular post-processing method, *Conformalized Quantile Regression* which is properly introduced in Section 3, improves the predictive performance for this model on a validation set by computing the Weighted Interval Scores for Covid-19 Cases and Covid-19 Deaths separately:

```
df_updated <- update_predictions(
  hub_germany,
  methods = "cqr", models = "EuroCOVIDhub-ensemble", cv_init_training = 0.5
)
df_combined <- collect_predictions(df_updated)

df_combined |>
  extract_validation_set() |>
  scoringutils::score() |>
  scoringutils::summarise_scores(by = c("method", "target_type"))
```

Table 1 shows that CQR improved the WIS for Covid-19 Cases, whereas the predictive performance for Covid-19 Deaths dropped slightly.

The `update_predictions()` and `collect_predictions()` combination immediately generalize to multiple post-processing methods. The only syntax change is a vector input of strings for the `methods` argument instead of a single string. Hence, if not desired, the user does not have to learn separate interfaces for

Table 1: Comparison of the Weighted Interval Score after CQR Adjustments

method	target type	interval score	dispersion
cqr	Cases	13.40	5.07
original	Cases	13.78	3.81
cqr	Deaths	0.06	0.01
original	Deaths	0.05	0.03

each method nor be familiar with the precise implementation. This design allows for maximum syntactic consistency by masking the internal functionality.

Further, the `update_predictions()` function automatically takes care of *quantile crossing* (Bassett and Koenker 1982) by reordering the output predictions in increasing quantile order. The `cv_init_training` parameter specifies the fraction of observations that is used for the pure training set before the Time Series Cross Validation process starts.

As seen in Table 1 CQR increases the *dispersion* of the predictions for Cases significantly. One example of these wider intervals is visualized in Figure 3.

```
plot_intervals(df_combined, target_type = "Cases", horizon = 2, quantile = 0.05)
```

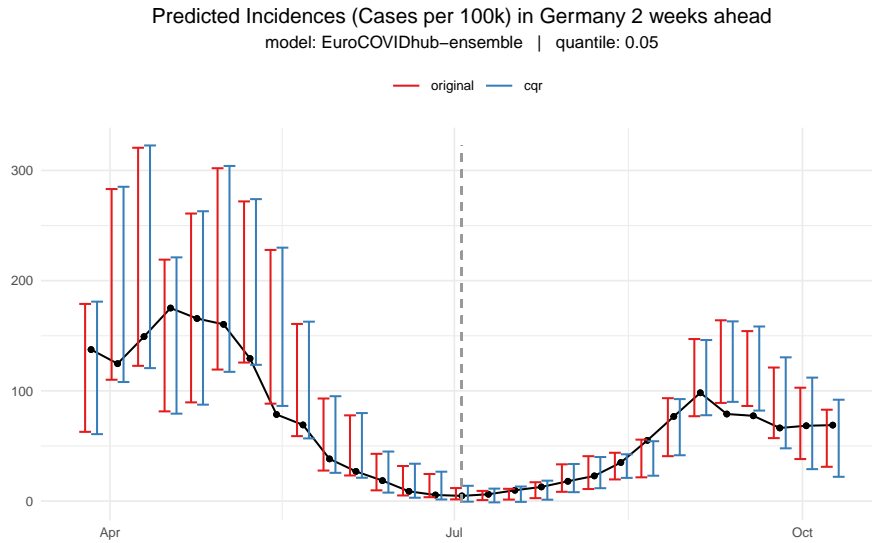


Figure 3: Original and CQR-adjusted Prediction Intervals for Covid-19 Cases in Germany

Indeed, the 2 weeks-ahead 90% prediction intervals for Covid Cases in Germany are widened by CQR. The grey dashed line indicates the end of the training set within the Cross Validation as specified by the `cv_init_training` parameter.

Recall from Figure 2 that prediction uncertainty increases with larger forecast horizons. Similarly, CQR *corrections* also increase in size for forecasts that are submitted further in advance, which can be seen in Figure 4 along the horizontal dimension. Interestingly, CQR expands the intervals only for Cases whereas the forecasts for Deaths are narrowed!

```
plot_intervals_grid(df_combined, facet_by = "horizon", quantiles = 0.05)
```

Besides the target type (Cases or Deaths), it is also useful to compare CQR effects across forecast horizons or quantiles. Quite intuitively, CQR generally has a stronger *relative* benefit for large time horizons and extreme quantiles, where the original forecaster faced a greater uncertainty. Figure 5 illustrates how, in special cases

Predicted Incidences (per 100k) in Germany
model: EuroCOVIDhub-ensemble | quantile: 0.05

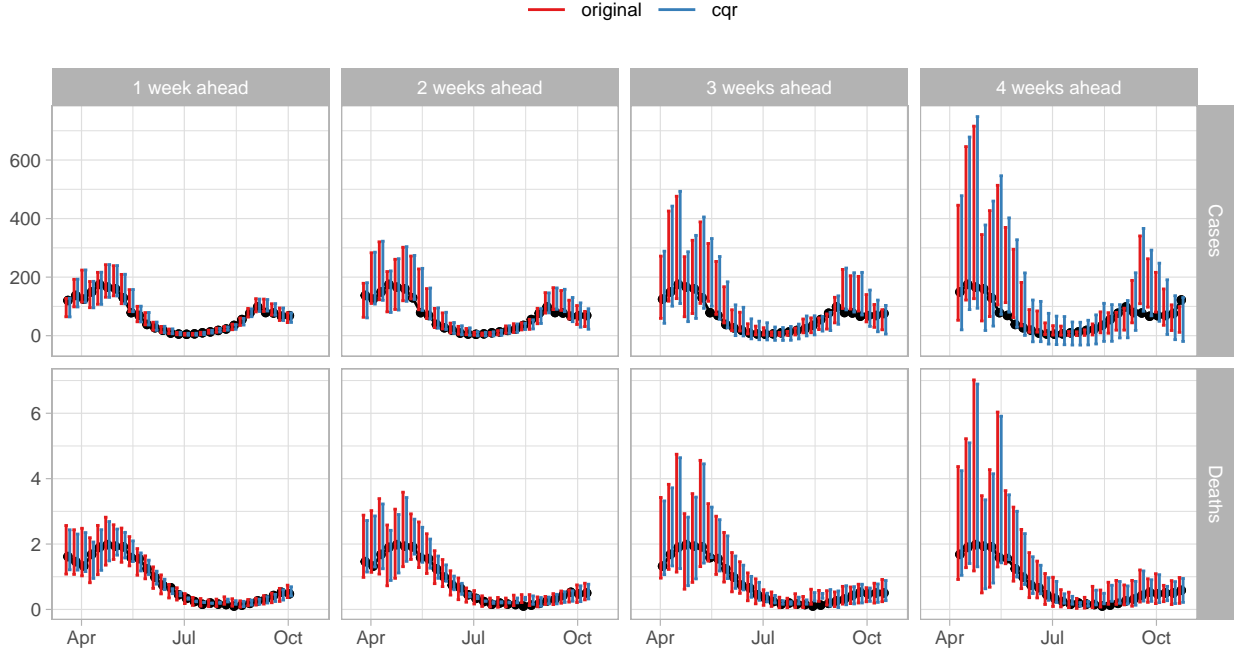


Figure 4: Original and CQR-adjusted Prediction Intervals for different Forecast Horizons

like this one, the effect on the validation set can show rather mixed trends due to disadvantageous adjustments for the two and three weeks-ahead 98% prediction intervals.

```
df_eval <- eval_methods(df_combined, summarise_by = c("quantile", "horizon"))
plot_eval(df_eval)
```

3 Conformalized Quantile Regression

This chapter introduces *Conformalized Quantile Regression* (CQR) as the first of two main Post-Processing procedures which are implemented in the `postforecasts` package.

Section 3.1 explains the original Conformalized Quantile Regression algorithm as proposed by Romano, Patterson, and Candès (2019). The underlying more general concept of *Conformal Inference* is motivated by Tibshirani (2019). We highlight potential limitations of the traditional implementation that could potentially be diminished by more flexible variants of CQR that are discussed in Section 3.2 and Section 3.3.

3.1 Traditional CQR

All derivations in this section are taken from the original paper (Romano, Patterson, and Candès 2019). The authors motivate Conformalized Quantile Regression by stating two criteria that the ideal procedure for generating prediction intervals should satisfy:

- It should provide valid coverage in finite samples without making strong distributional assumptions.
- The resulting intervals should be as narrow as possible at each point in the input space.

According to the authors CQR performs well on both criteria while being distribution-free and adaptive to heteroscedasticity.

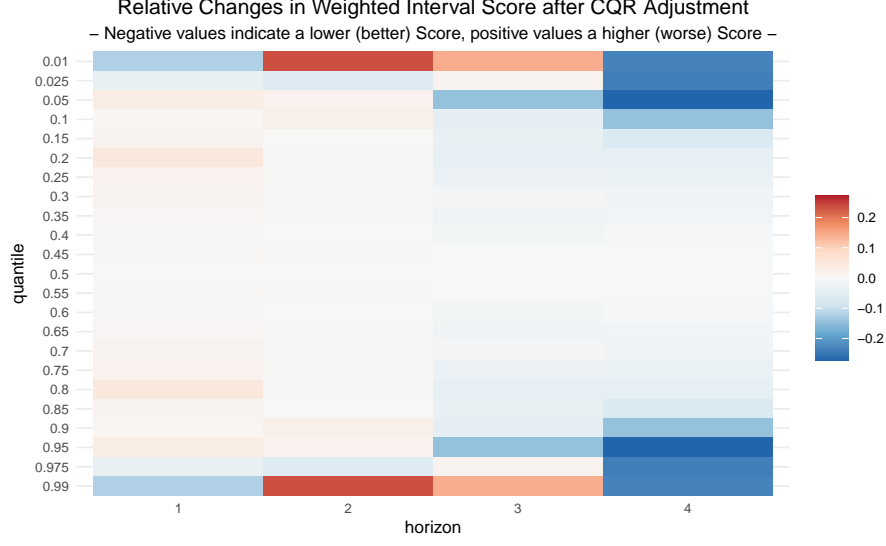


Figure 5: Relative Changes in the WIS through CQR for all Quantile-Horizon combinations

3.1.1 Statistical Validity

The algorithm that CQR is build upon is statistically supported by Theorem 3.1. The term *conformity scores* is defined in Section 3.1.2.

Theorem 3.1. *If $(X_i, Y_i), i = 1, \dots, n + 1$ are exchangeable, then the $(1 - \alpha) \cdot 100\%$ prediction interval $C(X_{n+1})$ constructed by the CQR algorithm satisfies*

$$P(Y_{n+1} \in C(X_{n+1})) \geq 1 - \alpha.$$

Moreover, if the conformity scores E_i are almost surely distinct, then the prediction interval is nearly perfectly calibrated:

$$P(Y_{n+1} \in C(X_{n+1})) \leq 1 - \alpha + \frac{1}{|I_2| + 1},$$

where I_2 denotes the calibration (validation) set.

Thus, the first statement of Theorem 3.1 provides a *coverage guarantee* in the sense that the adjusted prediction interval is *lower-bounded* by the desired coverage level. The second statement adds an *upper-bound* to the coverage probability which gets tighter with increasing sample size and asymptotically converges to the desired coverage level $1 - \alpha$ such that lower bound and upper bound are asymptotically identical.

3.1.2 Algorithm

The CQR algorithm is best described as a multi-step procedure.

Step 1:

Split the data into a training and validation (here called *calibration*) set, indexed by I_1 and I_2 , respectively.

Step 2:

For a given quantile α and a given quantile regression algorithm \mathcal{A} , compute the original lower and upper quantile predictions on the training set:

$$\{\hat{q}_{\alpha, low}, \hat{q}_{\alpha, high}\} \leftarrow \mathcal{A}(\{(X_i, Y_i) : i \in I_1\}).$$

Note that the algorithm does *not* make any assumptions about the structural form of \mathcal{A} which, in theory, could be a highly nonlinear function like a Deep Neural Network.

Step 3:

Compute *conformity scores* on the calibration set:

$$E_i := \max \{ \hat{q}_{\alpha,low}(X_i) - Y_i, Y_i - \hat{q}_{\alpha,high}(X_i) \} \quad \forall i \in I_2$$

Thus, for each i , the corresponding score E_i is *positive* if Y_i is *outside* the interval $[\hat{q}_{\alpha,low}(X_i), \hat{q}_{\alpha,high}(X_i)]$ and *negative* if Y_i is *inside* the interval.

Step 4:

Compute the *margin* $Q_{1-\alpha}(E, I_2)$ given by the $(1 - \alpha)(1 + \frac{1}{1+|I_2|})$ -th empirical quantile of the score vector E in the calibration set. For small sample sizes and small quantiles α this procedure might result in quantiles greater than 1. In this case we simply select the maximum value of the score vector.

Step 5:

On the basis of the original lower and upper quantile prediction $\hat{q}_{\alpha,low}(X_i)$ and $\hat{q}_{\alpha,high}(X_i)$, the new *post-processed* prediction interval for Y_i is given by

$$C(X_{n+1}) = [\hat{q}_{\alpha,low}(X_i) - Q_{1-\alpha}(E, I_2), \hat{q}_{\alpha,high}(X_i) + Q_{1-\alpha}(E, I_2)].$$

Note that the *same* margin $Q_{1-\alpha}(E, I_2)$ is subtracted from the original lower bound and added to the original upper bound. This limitation is addressed in Section 3.2.

3.1.3 Results

We now investigate how well the algorithm performs in the context of Covid-19 forecasts. Thereby we start with the UK Covid-19 Forecasting Challenge data set and point out general and recurrent trends of CQR updates. Then, we continue with a more detailed discussion of the findings for the larger European Forecast Hub data.

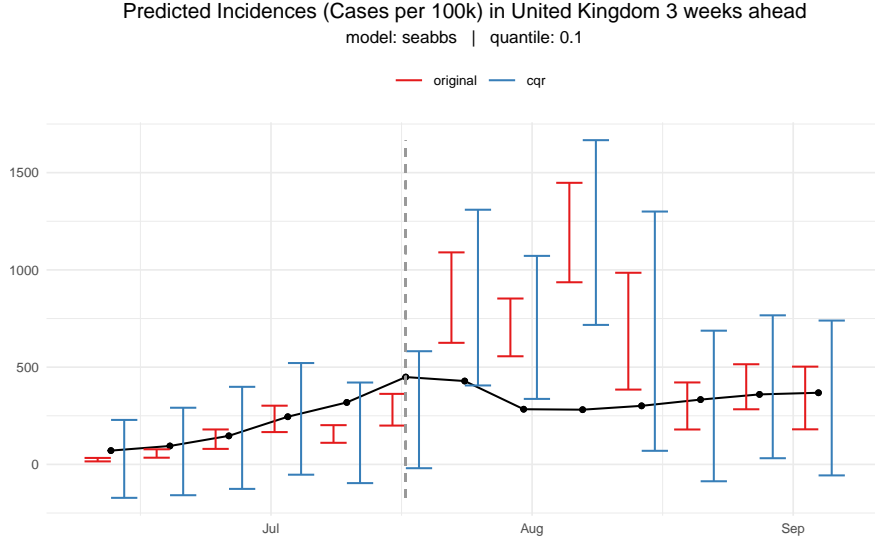


Figure 6: CQR tends to make prediction intervals larger, here for the `seabbs` forecasting model

As stated in Step 5 of Section 3.1.2 CQR moves the original lower and upper bounds *symmetrically* either inwards or outwards by using the *same* margin. This implies that the interval *midpoint* remains unchanged when applying the traditional CQR algorithm. One common characteristic that applies to almost all feature combinations is that CQR *widens* the original forecast intervals. One rather extreme example is shown in Figure 6. Since the `seabbs` forecasts are submitted by a single individual, we find evidence for the hypothesis of Section 2.1 that humans tend to be too confident in their own predictions resulting in too narrow uncertainty bounds. By extending the intervals symmetrically CQR maintains *pointwise* information from the original forecasts while simultaneously increasing interval coverage.

Table 2: WIS improvement by CQR for one particular feature combination on the validation set.

method	model	target type	horizon	quantile	interval score	dispersion
cqr	seabbs	Cases	3	0.1	157.32	87.49
original	seabbs	Cases	3	0.1	210.62	38.14

Table 3: Overall WIS improvement by CQR on the validation set.

method	interval score	dispersion
cqr	62.15	24.1
original	65.74	12.0

The pure effect of increasing coverage, however, does *not* automatically imply that the Weighted Interval Score has improved due to the trade-off between coverage and precision. Thus, we explicitly compute the WIS, first for the specific feature combination of Figure 6 in Table 2 and then aggregated over all *models*, *target types*, *horizons* and *quantiles* in Table 3.

Both tables confirm the visual impression of Figure 6: CQR improves the WIS by increasing the *dispersion* value, a measure for the interval *spread*. This effect is particularly strong in case of the **seabbs** model but still applies to a more moderate extent to most of the remaining forecasting models.

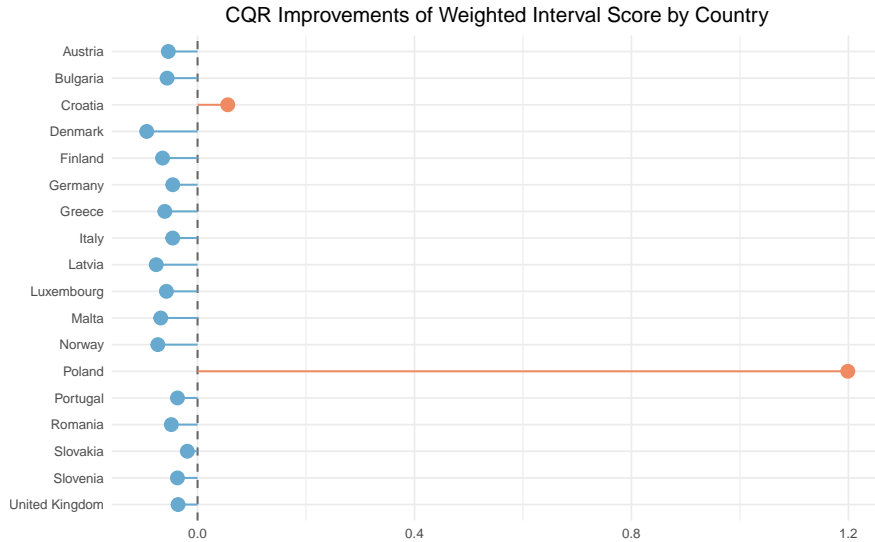


Figure 7: CQR proves to be beneficial for the vast majority of countries, with the major exception of Poland

Since many of the general findings for traditional CQR coincide between the UK data and the EU Forecast Hub data, we jump straight to the latter for the following analysis. First, we investigate if CQR is equally effective across all countries. Figure 7 indicates that this is clearly *not* the case: CQR is beneficial on out of sample data in almost all of the 18 selected countries. The largest effect size, however, is linked to Poland in *negative* direction.

At first sight this finding seems like a data entry error, there is no obvious reason why a generic algorithm like Conformalized Quantile Regression might not work for one specific location. The large negative effect is also interesting in light of Theorem 3.1: We know that CQR *always* improves the forecast intervals on the training set which, of course, applies to Poland as well. We can confirm this theoretical guarantee empirically by evaluating the WIS for Poland on the training set only. Table 4 collects the training and validation scores

Table 4: Weighted Interval Score for Poland by Model on Training and Validation Set

method	model	training score	validation score
cqr	epiforecasts-EpiNow2	22.84	1.94
original	epiforecasts-EpiNow2	23.71	1.32
cqr	EuroCOVIDhub-ensemble	29.44	2.34
original	EuroCOVIDhub-ensemble	31.37	0.96
cqr	IEM_Health-CovidProject	56.54	4.68
original	IEM_Health-CovidProject	62.04	0.91

for three selected forecasting models separately.

Indeed, CQR improves the WIS for all three models in-sample whereas the out-of-sample performance drops dramatically. This finding provides evidence that the observations used for the initial training phase must be *fundamentally different* to those encountered during the Cross Validation process. More specifically, it suggests a *distribution shift* of the true observed values and/or the original quantile predictions right at the split of training and validation phase. Further, the *scale* of training and validation scores is quite different, which usually stems from different magnitudes of the observed incidences within each stage.

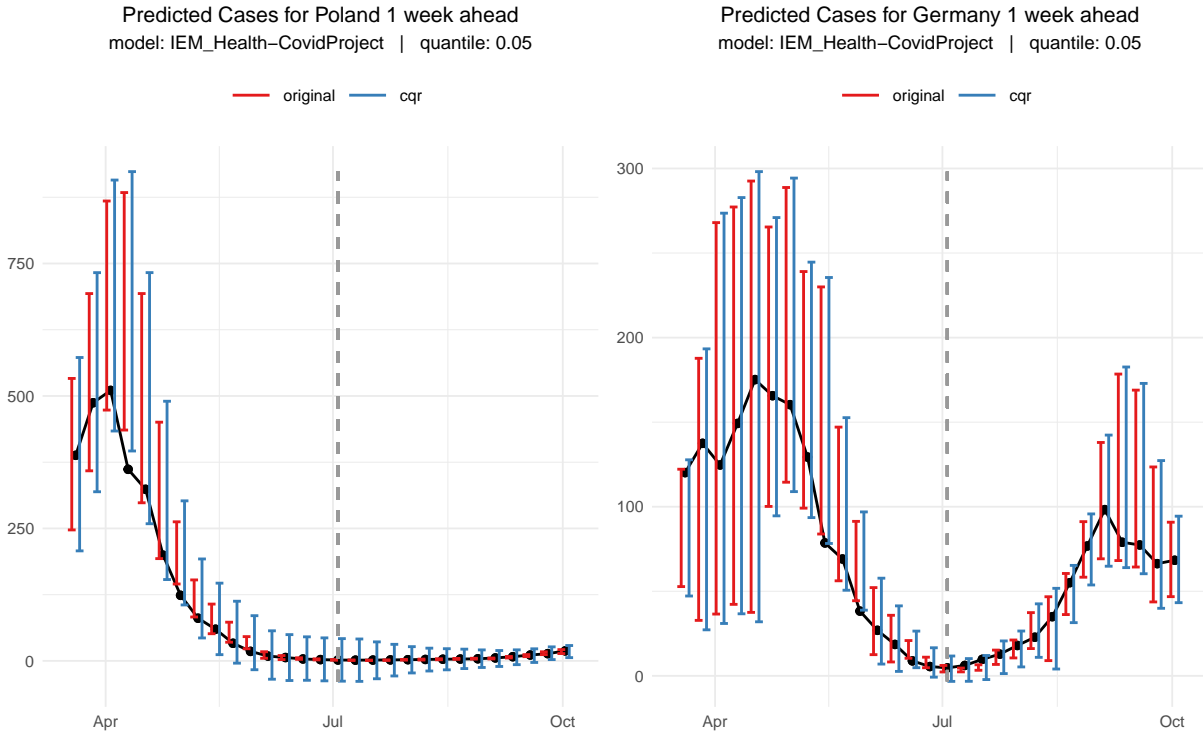


Figure 8: Development of Covid-19 Cases in 2021 in Poland and Germany

Figure 8 confirms our hypothesis for 1 week-ahead forecasts of 90% prediction intervals for Covid-19 Cases. The plots display the development of observed and predicted values for the outlier Poland (left) compared to the same setting for Germany (right) where CQR performs just fine. A few weeks before the training-validation split, which is highlighted by the grey dashed line, the true incidences plummeted in Poland. In strong contrast to Germany, where the Covid-19 situation relaxed during the summer months of 2021 as well, the incidences *remain* low until late autumn in Poland (according to the collected data of the European Forecast Hub). Thus, the incidences are indeed much lower on average in the validation set which explains the scale

discrepancy in Table 4.

The consistently low incidences are connected to decreased uncertainty margins of the original forecasts that were submitted only one week in advance. The forecasters were well aware of the current Covid-19 situation and were able to quickly react with reduced point forecasts and narrower prediction intervals. CQR is not capable of competing with this flexibility and requires a long time span to adapt to irregular behaviour. The reasons for these slow adjustments, which reveal a major downside of CQR, follow immediately from the underlying statistical theory. Section 3.2.2 explains this connection in detail.

Lastly, we summarize the performance of vanilla CQR across different *quantiles*, *target types* and *horizons*. To obtain more informative visual illustrations we exclude Poland from the further analysis.

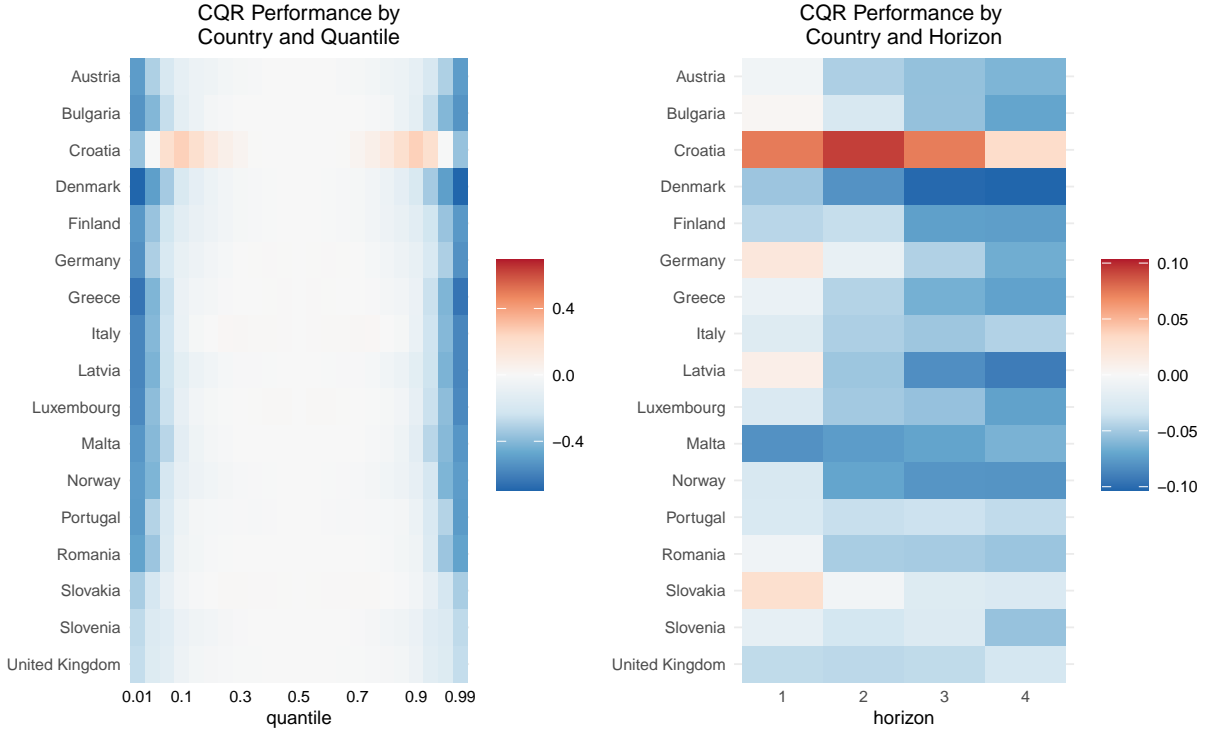


Figure 9: CQR is most beneficial for extreme Quantiles and large Forecast Horizons

The left plot of Figure 9 shows the performance of CQR for all 23 quantile levels in the data set. Although the effect size varies by country, the general trend holds unanimously: Extreme quantiles in the tails of the predictive distribution benefit most from post-processing with a gradual decline towards centered quantiles. The same trend can be observed to an even larger extent for non-expert forecasts in the UK Covid-19 Forecasting Challenge data set.

Similar to quantiles there exist obvious tendencies for different forecast *horizons* as well. The right plot of Figure 9 shows the performance of CQR across horizons, again stratified by country. Although the effects are more diverse compared to the analysis across quantiles, CQR generally works better for larger forecast horizons. Exceptions of this rule are Croatia, which is the only country besides Poland with a negative total effect of CQR, and Malta, where the trend is actually reversed and CQR updates are most beneficial for short-term forecasts.

Both of the previous figures suggest that post-processing with Conformalized Quantile Regression is worthwhile whenever the uncertainty is comparably high, e.g. for quantiles in the tails of the distribution or large forecast horizons.

Lastly, Table 5 aggregates the WIS on the validation set by *target type*. Interestingly, the effect *directions* disagree for the first time: Forecasts for Covid-19 Cases benefit significantly whereas there is no significant

Table 5: CQR Improvements by Target Type for European Forecast Hub Data excluding Poland

method	target type	interval score	dispersion
cqr	Cases	59.26	19.55
original	Cases	62.69	15.49
cqr	Deaths	0.32	0.15
original	Deaths	0.32	0.13

impact on forecasts for Covid-19 Deaths.

3.2 Asymmetric CQR

3.2.1 Theory

This section proposes a first extension to the original CQR algorithm by relaxing the symmetry assumption. Instead of limiting ourselves to choose the *same* margin $Q_{1-\alpha}(E, I_2)$ on a *single* score vector E for adjusting the original lower and upper quantile predictions, we allow for individual and, thus, generally different margins $Q_{1-\alpha,low}(E_{low}, I_2)$ and $Q_{1-\alpha,high}(E_{high}, I_2)$ such that the post-processed prediction interval is given by

$$C(X_{n+1}) = [\hat{q}_{\alpha,low}(X_i) - Q_{1-\alpha,low}(E_{low}, I_2), \hat{q}_{\alpha,high}(X_i) + Q_{1-\alpha,high}(E_{high}, I_2)].$$

This asymmetric version additionally requires a change in the computation of the conformity scores. Instead of considering the elementwise maximum of the differences between observed values Y_i and original bounds, we simply compute two separate score vectors:

$$\begin{aligned} E_{i,low} &:= \hat{q}_{\alpha,low}(X_i) - Y_i \quad \forall i \in I_2 \\ E_{i,high} &:= Y_i - \hat{q}_{\alpha,high}(X_i) \quad \forall i \in I_2 \end{aligned}$$

3.2.2 CQR Downsides

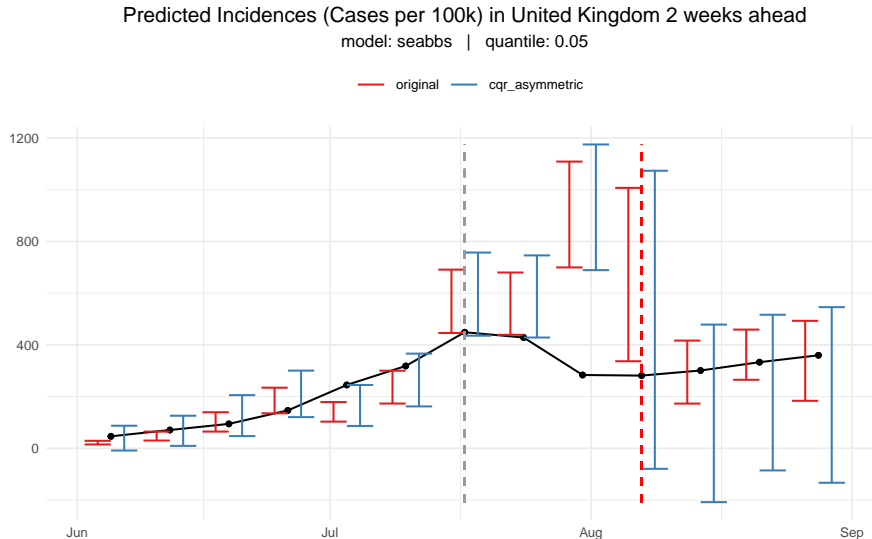


Figure 10: Illustration of CQR's slow reaction process

Figure 10 nicely demonstrates the key characteristics of asymmetric CQR: Adjustments of the lower and upper interval bounds are independent from each other. Considering the last interval on the far right the lower bound is adjusted downwards by a large amount whereas the upper bound is only slightly increased.

This behaviour implies that, contrary to traditional CQR, original and updated prediction intervals are generally *not* centered around the same midpoint.

The plot also illustrates what we have already seen in Section 3.1: Once the true value is not contained in the prediction interval and there is a large discrepancy towards the closest boundary, all CQR versions tend to *overcompensate* in the next time step. This jump can be observed from time step 9 to time step 10, where the latter is highlighted by the red dashed line. Even more problematic, the large correction margin only vanishes very gradually afterwards even if the observed Time Series has stabilized. In Figure 10 the lower quantile prediction of asymmetric CQR approaches the original lower quantile forecast very slowly after the jump in observed Cases. The following paragraphs aim to explain this inflexibility in detail and draw the connection to the underlying statistical algorithm of Section 3.1.2.

Going back to Section 3.2.1 asymmetric CQR computes two separate score vectors based on the original lower and upper quantile forecasts and the vector of observed values. To confirm our findings visually we now focus on the data subset of Figure 10.

Consider the intervals one step prior to the dashed red line. At this point in time the training set includes the first 9 elements of true values and predicted quantiles which are then used to compute a list of lower and upper scores:

```
scores_list <- compute_scores_asymmetric(
  true_values[1:9], quantiles_low[1:9], quantiles_high[1:9]
)
scores_list$scores_lower
## [1] -31.443366 -40.808821 -29.765120 -11.289450 -141.757533 -145.173165
## [7] -2.839344 10.514219 415.998372
```

The vector of lower scores E_{low} is given by $\hat{q}_{\alpha,low}(X) - Y$, i.e. by elementwise differences of true values and predicted lower quantiles at each time step. Due to the jump from time point 9 to 10 the final element of the lower score vector has a large value of around 416.

Next, the (scalar) lower margin $Q_{1-\alpha,low}(E_{low})$ is computed:

```
margin <- compute_margin(scores_list$scores_lower, quantile)
margin

##      100%
## 415.9984
```

Due to the small sample size of 9 observations and the relatively small quantile level of 0.05 the margin is simply the *maximum* or 100% quantile of the lower scores. The *updated* lower quantile prediction for the 10th time point is simply $\hat{q}_{\alpha,low}(X_{10}) - Q_{1-\alpha,low}(E_{low})$, i.e. the original lower quantile prediction at time point 10 minus the margin:

```
quantiles_low[10] - margin

## [1] -79.18
```

which coincides with Figure 10.

The procedure now continues by consecutively adding the next elements to the vector of true values and original quantile predictions. Since the differences of observed incidences and predicted lower bounds are all much smaller for the remaining time steps, the *same* value 416 remains the maximum of the lower score vector until the end! Thus, if just like in the case above, the margin always equaled the maximum score, the adjustments would remain that large independent of the future development of the time series.

In fact, the only difference from that scenario to Step 4 of Section 3.1.2 is that the quantile of the score vector, which determines the value of the margin, depends on the *size* of the score vector. Since the size increases by one with each time step during the Cross Validation process, this quantile slowly declines. For instance, the margin which is responsible for adjusting forecasts at time point 11 is not simply the maximum anymore:

Table 6: Performance of asymmetric CQR on Validation Set

method	uk interval score	hub interval score
cqr_asymmetric	63.97	34.37
original	65.74	29.84

```
scores_list <- compute_scores_asymmetric(
  true_values[1:10], quantiles_low[1:10], quantiles_high[1:10]
)
margin <- compute_margin(scores_list$scores_lower, quantile)
margin
```

```
##      99%
## 383.5547
```

In this case the 99% quantile is a linear interpolation of the largest and second largest score, as implemented by the `stats::quantile()` function. Hence, even though the score outlier is not selected directly, it strongly impacts the margins of future time steps.

The cycle proceeds in this way until the end. The conclusion of this case study is that all modifications of the traditional CQR algorithm suffer from a slow reaction time towards distribution shifts and particularly sudden jumps within observed values and original forecasts. This major downside of CQR is an immediate consequence of the *margin* computation which ultimately determines the magnitude of forecast corrections

3.2.3 Results

Contrary to traditional CQR, the effect of asymmetric CQR highly depends on the underlying data set. Table 6 shows that the asymmetric version is beneficial for the UK data set by improving the out-of-sample Weighted Interval Score, yet the opposite is the case for the European Forecast Hub.

To get a better intuition which circumstances contribute to a positive or negative outcome, we analyze the effects in more granularity. Figure 12 illustrates the relative improvements by asymmetric CQR for different forecasting models and different forecast horizons stratified by the quantile level for the UK data. We exclude the `EuroCOVIDhub-baseline` model where the adjustments uniformly lead to a much *worse* score.

The general trends are similar to vanilla CQR: Areas of higher uncertainty profit more from post-processing. While the effect is still positive for quantiles less than 0.15 or greater than 0.85, the *original* predictions are more accurate for centered quantiles across all models. The same statement holds for three or four week-ahead predictions. For short term forecasts, however, the effect is negative across *all* quantile levels.

Recall that traditional CQR improved performance for almost all European countries with the huge outlier Poland where the opposite effect could be observed. In light of the discussion in Section 3.2.2 it is not surprising that Poland keeps its outlier role for asymmetric CQR as well, since the slow reaction process to distribution shifts is coupled with the core of the CQR algorithm and not diminished by merely relaxing the symmetry assumption. In contrast to Figure 7, however, the relative effect of asymmetric CQR is *negative* for almost all of the remaining countries.

Thus, we detect first evidence that the (at least partially) promising results for the smaller UK data set do *not* transfer to the larger European Forecast Hub in this case. Figure 13 convincingly shows that the performance indeed dropped for each quantile and horizon category. While the asymmetric updates still result in slightly better predictions for intervals with large nominal coverage level, the left plot is dominated by the negative effect for centered quantiles, except for the median prediction which remains untouched by all CQR versions. The right plot suggests that corrections with asymmetric CQR should be avoided altogether when only grouping by forecast horizons and not considering quantile levels separately.

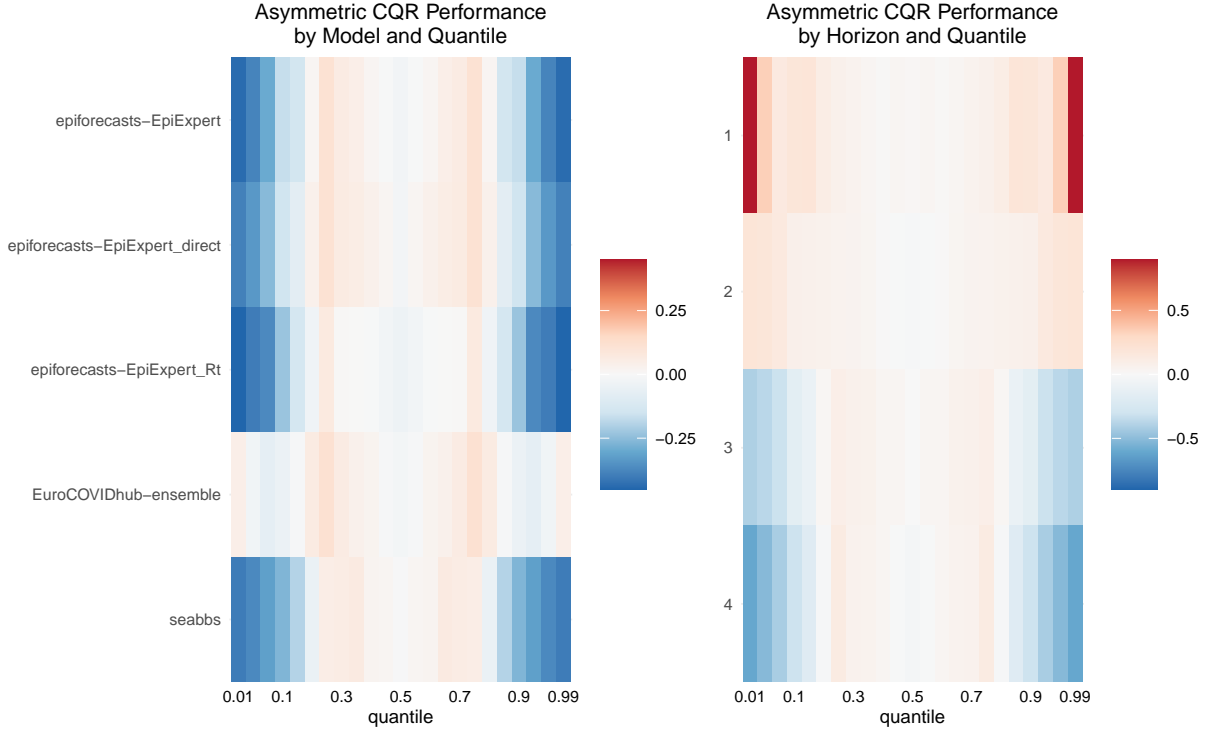


Figure 11: Mixed Results of asymmetric CQR on UK data

Table 7: Performance of asymmetric CQR for Covid-19 Cases and Deaths

method	target type	uk interval score	hub interval score
cqr_asymmetric	Cases	127.78	70.59
original	Cases	131.29	62.69
cqr_asymmetric	Deaths	0.16	0.50
original	Deaths	0.18	0.32

Finally, Table 7 summarizes the dissimilar effects on the two data sets very clearly: Aggregated over all other categories, asymmetric CQR *does* improve the WIS for Covid-19 Cases and Deaths in the UK data. In strong contrast, the post-processed intervals perform *much* worse than the original forecasts across both target types in the European Forecast Hub data set.

In conclusion, asymmetric Conformalized Quantile Regression can lead to improved prediction intervals as it is the case for the UK data set. However, the vast majority of countries in the European Forecast Hub do not benefit from this first CQR modification. Compared to the traditional CQR algorithm, giving up on symmetry leads to a worse performance across both data sets. It is worth noting that allowing for separate lower and upper margins does *not* cause significant overfitting as one might assume, the original CQR algorithm outperforms the asymmetric version even on the training set! This finding, however, only holds for the European Forecast Hub, a more detailed comparison of the two CQR versions for the UK data can be found in Section 5.

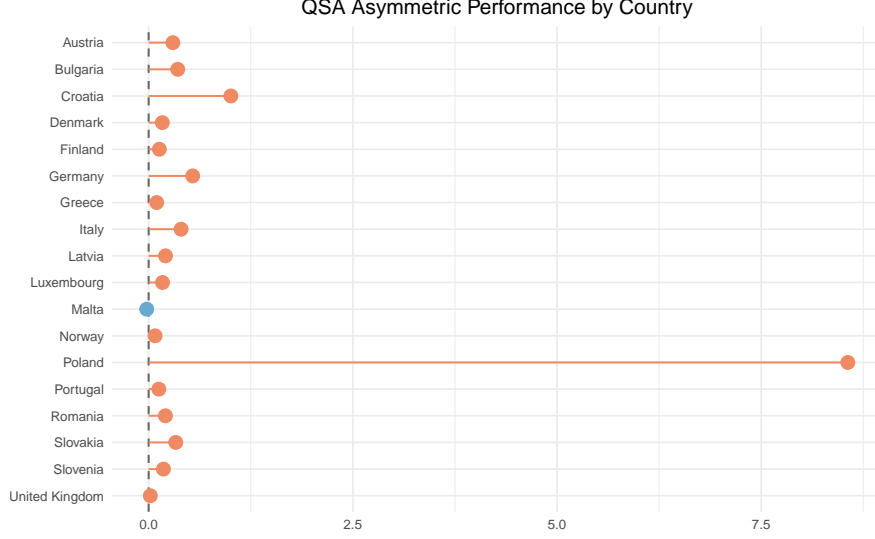


Figure 12: Asymmetric CQR has negative effects on almost all countries

3.3 Multiplicative CQR

3.3.1 Theory

On top of the asymmetric CQR modification described in Section 3.2, we can extend the CQR algorithm further. So far, the adjustments to the original prediction interval were always chosen in *additive* form. It may be useful to leverage the *magnitude* of the original bounds more explicitly by using *relative* or *multiplicative* adjustments.

Hence, we again compute separate margins $Q_{1-\alpha,low}(E_{low}, I_2)$ and $Q_{1-\alpha,high}(E_{high}, I_2)$ which are now *multiplied* with the existing forecasts. The post-processed prediction interval is thus given by

$$C(X_{n+1}) = [\hat{q}_{\alpha,low}(X_i) \cdot Q_{1-\alpha,low}(E_{low}, I_2), \hat{q}_{\alpha,high}(X_i) \cdot Q_{1-\alpha,high}(E_{high}, I_2)].$$

Similar to the asymmetric additive version, the computation of the score vectors is changed accordingly to respect the new multiplicative relationship:

$$E_{i,low} := \frac{Y_i}{\hat{q}_{\alpha,low}(X_i)} \quad \forall i \in I_2$$

$$E_{i,high} := \frac{Y_i}{\hat{q}_{\alpha,high}(X_i)} \quad \forall i \in I_2,$$

where we have to exclude original predictions with the value 0. Since all Covid-19 Cases and Deaths are non-negative, we threshold the scores at zero such that $E_{i,low}$ equals 0 whenever $\hat{q}_{\alpha,low}(X_i) \leq 0$.

Note that the actual limiting value

$$\lim_{\hat{q}_{\alpha,low}(X_i) \rightarrow 0} \frac{Y_i}{\hat{q}_{\alpha,low}(X_i)} = \infty$$

does *not* make sense here since infinite scores would cause infinite lower margins $Q_{1-\alpha,low}(E_{low}, I_2)$, which in return result in infinite updated lower bounds. Thus, the value 0 is deliberately chosen to minimize the influence of negative original forecasts and keep the updated lower quantile predictions always nonnegative.

3.3.2 Regularization

While the idea of multiplicative correction terms is appealing, it turns out that the approach above is flawed in two ways:

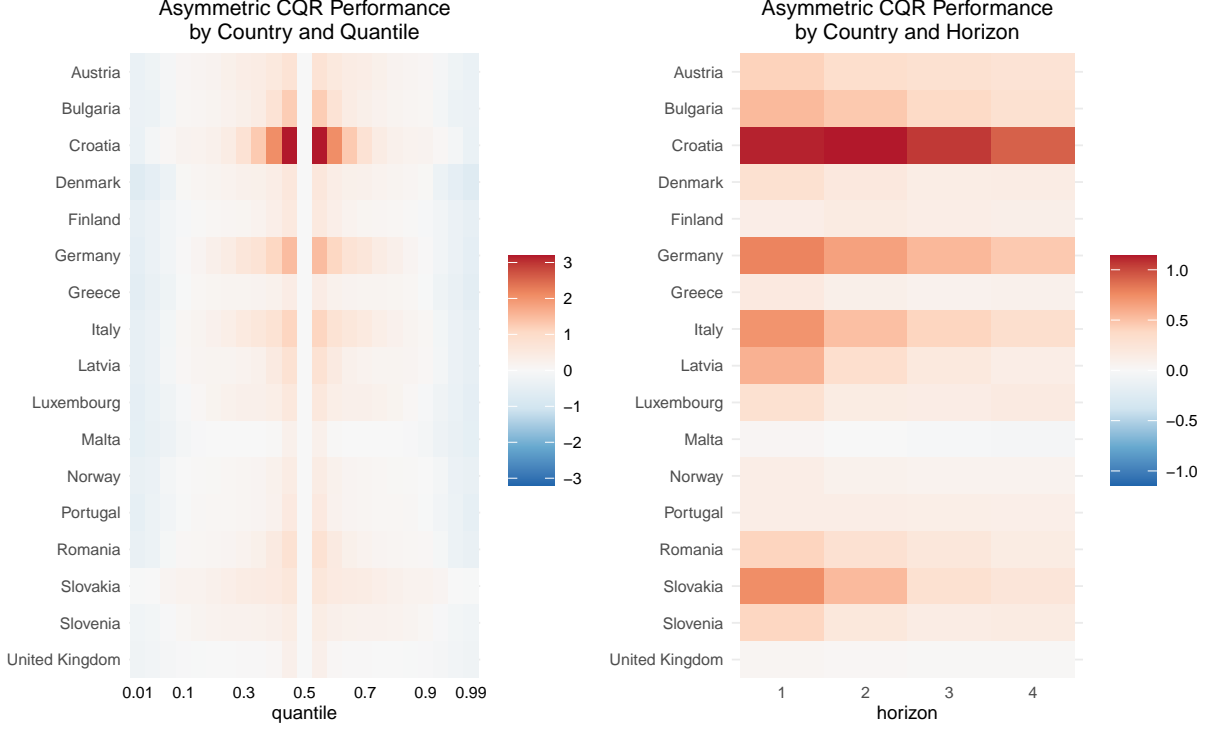


Figure 13: Out-of-sample performance of asymmetric CQR on European Forecast Hub data

1. Recall that the (lower) margin $Q_{1-\alpha,low}(E_{low}, I_2)$ basically *picks* a value of the score vector E_{low} at a given quantile level. The score vectors are computed for each combination of *location*, *model*, *target type*, *horizon* and *quantile*, i.e. the number of values in the score vector is identical to the number of distinct time points in the training set. For short time series such as our small UK data set, the margin selects the *largest* value in the score vector for small levels of α such as 0.01 or 0.05, where each such value represents a *ratio* of observed Y_i and original prediction $\hat{q}_{\alpha,low}(X_i)$.

As one might guess, these factors frequently get very large for small initial quantile predictions $\hat{q}_{\alpha,low}(X_i)$ such that the computed margin $Q_{1-\alpha,low}(E_{low}, I_2)$ for post-processing is unreasonably large. In fact, the margin can remain huge if there exists a *single* outlier in the score vector. In particular, this naive multiplicative version frequently adjusts the lower quantile prediction to a higher value than its upper quantile counterpart, leading to (an extreme form of) quantile crossing.

We counteract this sensitivity to outliers by *reducing the spread* of the score vector. Since we deal with multiplicative factors it makes no sense to standardize them to zero mean and unit variance. Instead, we regularize the score vector by pulling all values closer to 1, while keeping all values nonnegative and respecting their *directions*, i.e. values smaller than 1 remain smaller than 1 and prior values greater than 1 remain greater than 1.

This goal is achieved by a *root transformation*. Since a greater spread of the score vector should lead to stronger regularization we settled on the corrections

$$E_{i,low}^{reg} = E_{i,low}^{\left(\frac{1}{\sigma_{E_{low}}}\right)}, \quad E_{i,high}^{reg} = E_{i,high}^{\left(\frac{1}{\sigma_{E_{high}}}\right)},$$

where σ_E denotes the standard deviation of the corresponding score vector.

Remark: We first restricted the scaling to the case $\sigma_{E_{low}}, \sigma_{E_{high}} > 1$, i.e. the spread of the score vector should only get reduced. However, the above correction empirically proved to be beneficial even for $\sigma_{E_{low}}, \sigma_{E_{high}} < 1$ in which case the score variance gets *increased*. Therefore we removed the original

restriction and only handled the (unlikely) case of constant score vectors with $\sigma_{E_{low}} = 0$ or $\sigma_{E_{high}} = 0$ separately.

2. Chances are high that at least *one* of the original true values Y_i is larger than its corresponding lower quantile prediction $\hat{q}_{\alpha,low}(X_i)$ such that the maximum of the (regularized) score vector is still larger than 1. Thus, the lower bound for small quantiles α is almost *always* pushed upwards. The same logic applies to the upper bound in which case the *entire interval* is shifted to the top. This behaviour is usually not desired.

To prevent interval shifts, we add the additional constraint that the lower and upper margin must multiply to 1, i.e.

$$Q_{1-\alpha,low} \cdot Q_{1-\alpha,high} \stackrel{!}{=} 1.$$

Hence, when the *lower* bound is adjusted upwards ($Q_{1-\alpha,low} > 1$), the upper bound must decrease ($Q_{1-\alpha,high} < 1$) and the interval becomes smaller. Similarly, when the *upper* bound is adjusted upwards ($Q_{1-\alpha,high} > 1$), the lower bound must decrease ($Q_{1-\alpha,low} < 1$) leading to larger intervals overall after post-processing.

3.3.3 Results

As noted in Section 3.3.2, *naive* multiplicative Conformalized Quantile Regression without any regularization is useless for updating quantile predictions. Typically, one would observe strong overfitting on the training set such that the training performance indicated promising effects, yet the scores on the validation set would be *much* worse than the original forecasts. Further, the adjusted intervals would be shifted upwards and usually be too large.

Before numerically evaluating the performance of *regularized* CQR, it is instructive to look at a visual comparison of all three CQR modifications for one specific feature combination as shown in Figure 14.

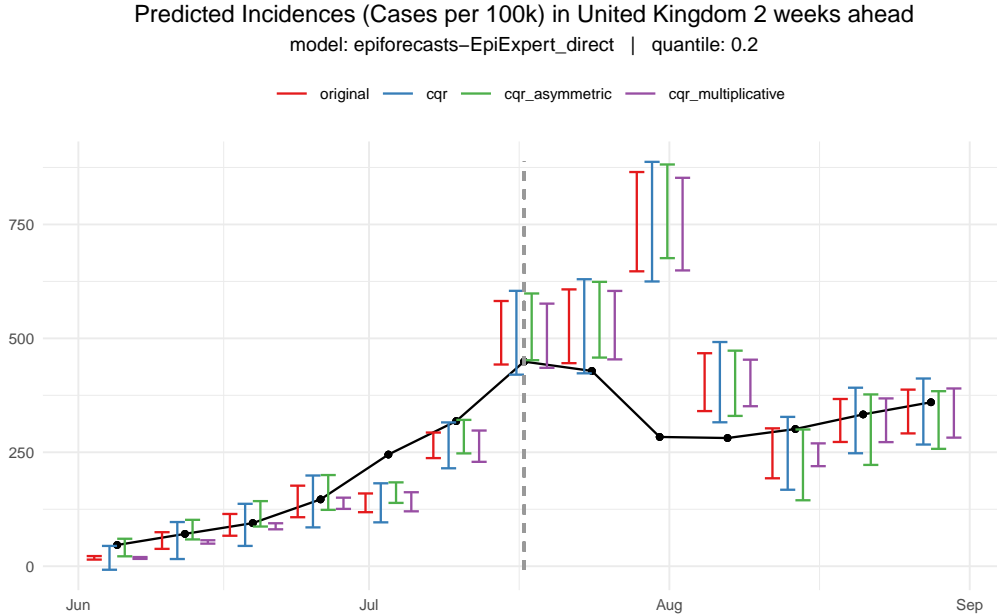


Figure 14: Comparison of CQR variations on the UK data set

The effect of scaling the score vectors in step one of the regularization procedure and constraining lower and upper margins in the second step can be detected immediately: Similar to vanilla CQR, the multiplicatively corrected intervals are now centered around the same midpoint as the original forecasts. In strong contrast to the additive CQR versions, however, the issue of interval explosion has not only been diminished by

Table 8: Performance of Multiplicative CQR on the Training Set

method	interval score	dispersion	underprediction	overprediction
cqr_multiplicative	24.49	5.98	18.01	0.51
original	23.62	4.16	18.88	0.58

Table 9: Performance of Multiplicative CQR by Model on the Validation Set

method	model	interval score	dispersion
cqr_multiplicative	epiforecasts-EpiExpert	71.60	10.05
original	epiforecasts-EpiExpert	67.74	12.07
cqr_multiplicative	EuroCOVIDhub-baseline	29.85	17.95
original	EuroCOVIDhub-baseline	29.61	5.92
cqr_multiplicative	EuroCOVIDhub-ensemble	61.24	15.48
original	EuroCOVIDhub-ensemble	56.07	14.00
cqr_multiplicative	seabbs	98.18	9.14
original	seabbs	95.11	14.03

downscaling the scores, but rather *reversed* such that the interval widths now actually *decreased* at most time points and generally appear too narrow.

Moreover, we no longer have any theoretical guarantees of improved forecasts on the training set since Theorem 3.1 only applies to the original additive and symmetric version of CQR. This fact is confirmed empirically by Table 8 which shows the Weighted Interval Score aggregated over all categories of `model`, `target_type`, `horizon` and `quantile`. Indeed, the multiplicative adjustments result in a slightly worse WIS on the training set.

Recall that this behaviour is different from the unregularized version, which performed better in-sample than the original forecasts across almost all feature combinations. On the flipside, the out-of-sample performance improved dramatically compared to the naive implementation, even though it ultimately does *not* lead to a score improvement for any of the selected forecasting models as shown in Table 9. Interestingly, multiplicative CQR indicates the best *relative* performance for the `EuroCOVIDhub-baseline` model where the additive CQR algorithms struggle the most. Overall the score differences across different forecasting models appear to be smoothed out compared to the previous CQR versions which also results from the regularization component that is unique to the multiplicative modification.

The impression of too narrow adjusted intervals does not generalize to the entire data set. The *dispersion* column in Table 9 shows that the intervals are downsized only for some models such as `epiforecasts-EpiExpert` whereas for others like `epiforecasts-ensemble` the distance between lower and upper bound gets larger on average.

Table 10 indicates a connection of the dispersion change by multiplicative CQR with the `quantile` level. Aggregated over all models, target types and horizons the dispersion value is increased by a large amount for extreme quantiles but remains in a similar range as before for quantiles in the center of the predictive

Table 10: Dispersion of Multiplicative CQR by Quantile on the Validation Set

method	0.01	0.025	0.05	0.1	0.15	0.2	0.25	0.3	0.35	0.4	0.45
cqr_multiplicative	8.79	7.40	11.98	16.83	18.26	18.82	18.24	17.53	14.60	10.12	5.22
original	2.82	5.82	9.65	14.86	17.84	18.99	18.83	17.44	14.71	10.97	6.08

distribution. This behaviour is in line with the previously seen additive correction methods and emphasizes that Figure 14 is not representative for the entire UK data set.

Overall, we must conclude that the original CQR algorithm as described by Romano, Patterson, and Candès (2019) can *not* be modified towards multiplicative margins in any straightforward way. For this reason, we neither extend the analysis of multiplicative CQR to the European Forecast Hub data set nor include it in the method comparison in Section 5.

4 Quantile Spread Adjustment

The general idea behind Quantile Spread Adjustment (QSA) is to adjust the spreads of each forecasted quantile by some factor. Quantile spreads are defined as the distance between the respective quantile and some basis. Three different points in the forecasting spectrum, intuitively make sensible basis: the median, the next inner neighbor and the symmetric interval quantile. The quantile spread for these different bases are illustrated in Figure 15.

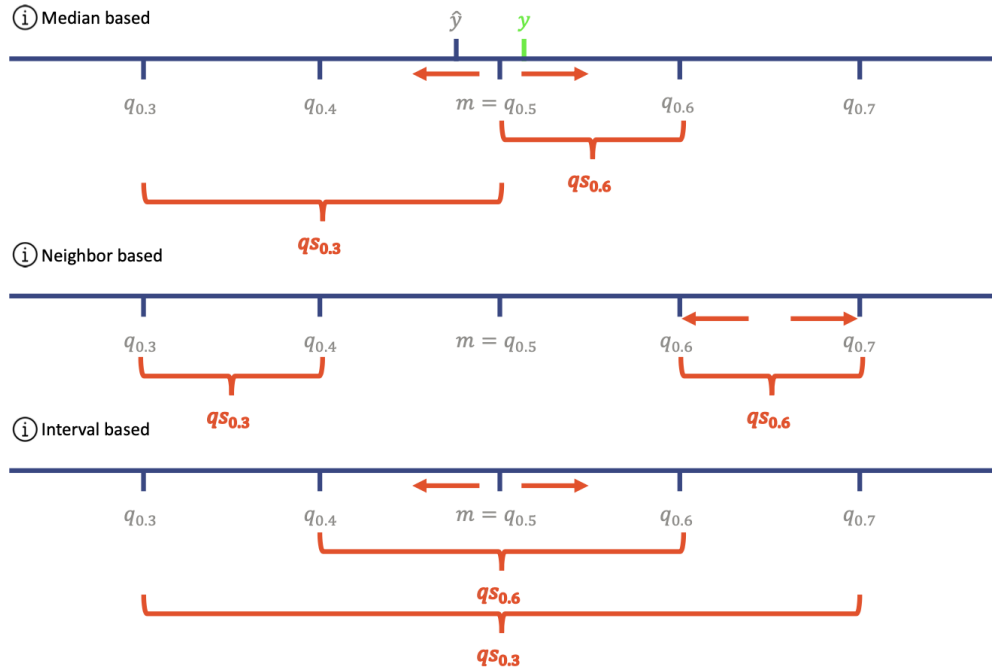


Figure 15: Quantile Spreads for different Basis

We choose the median based definition of the quantile spreads for two main reasons. First, in contrast to the neighborhood based definition, the median basis has the advantage that different quantile spreads are independent of each other. This property makes finding the optimal quantile spread adjustments for a large set of quantiles much simpler. It comes at the cost, however, that adjustments might lead to *quantile crossing*⁶, which would not be the case for neighborhood based adjustments. Our second reason to use the median basis is that, unlike the interval based approach, it does not restrict adjustments for quantile pairs to be symmetric.

4.1 Theory

Using the median based definition, the next step is to determine how to optimally adjust the quantile spreads. As target function, QSA uses the Weighted Interval Score from Section 2.1.3. Equation 1 shows how the

⁶As discussed in Section 2.2.2 `update_predictions()` automatically takes care of quantile crossing by reordering the output predictions in increasing quantile order

QSA weights \mathbf{w} influence the WIS, where p denotes the number of confidence intervals, α_p the certainty level of a confidence interval and n the number of observations.

$$\begin{aligned} \mathbf{w}^* &= \arg \min_{\mathbf{w} \in \mathbb{R}^p} WIS(\mathbf{y}) \\ &= \arg \min_{\mathbf{w} \in \mathbb{R}^p} \sum_{i=1}^p \frac{\alpha_i}{2} \sum_{j=1}^n (u_{i,j}^* - l_{i,j}^*) + \frac{2}{\alpha_i} \cdot (l_{i,j}^* - y_j) \cdot \mathbf{1}(y_j \leq l_{i,j}^*) + \frac{2}{\alpha_i} \cdot (y_j - u_{i,j}^*) \cdot \mathbf{1}(y_j \geq u_{i,j}^*) \quad (1) \\ \text{s.t.} \quad & l_{i,j}^* = l_{i,j} + (l_{i,j} - m) \cdot (w_i^l - 1) \quad \text{and} \quad u_{i,j}^* = u_{i,j} + (u_{i,j} - m) \cdot (w_i^u - 1) \end{aligned}$$

By varying the QSA factor w_i^l for the lower and w_i^u for the upper bound of a given prediction interval level α_i , QSA moves the quantiles from their original $l_{i,j}$ and $u_{i,j}$ to their updated values $l_{i,j}^*$ and $u_{i,j}^*$. QSA factors larger than 1 lead to an *increased* prediction interval, thus $w_i^l > 1$ reduces the value of $l_{i,j}^*$ and $w_i^u > 1$ increases the value of $u_{i,j}^*$.

These changes have two effects: On the one side an increase in w_i^l and w_i^u reduces the sharpness and increases the WIS, on the other side the increased interval may capture more observation which reduces the under- and overprediction penalties in the WIS. Thus depending on the positions of the observed values and predicted quantiles, QSA will either increase or decrease the interval size in order to minimize the WIS.

The `postforecasts` package implements the QSA optimization in three flavors that differ in the restriction of the weight vector \mathbf{w} : `qsa_uniform`, `qsa_flexible_symmetric` and `qsa_flexible`. These are listed in Equation 2.

$$\begin{aligned} \text{uniform} : w_i &= c \quad i \in [0, 1, \dots, p-1, p], \quad c \in \mathbb{R} \\ \text{flexibel_symmetric} : w_i &= w_{p-i} \quad i \in [0, 1, \dots, \frac{p}{2} - 1], \quad w_i \in \mathbb{R} \\ \text{flexible} : \mathbf{w} &\in \mathbb{R}^p \end{aligned} \quad (2)$$

`qsa_uniform` restricts all weight vector values to be identical. `qsa_flexible_symmetric` only restricts pairwise adjustments to be identical. It essentially represents unrestricted QSA with interval based adjustments. Finally, `qsa_flexible` is completely unrestricted as each quantile is adjusted separately.

In addition to different flavors, the `postforecasts` package also provides the option to regularize the optimization. Equation 3 displays the penalization term that is added to the WIS. It is designed to penalize differences between weight vector values by adding a factor proportional to the sum of squared deviations of the weight vector values from their mean. It therefore regularizes towards the `qsa_uniform` method and only has an effect for the `qsa_flexible_symmetric` and `qsa_flexible` flavors.

$$\begin{aligned} \mathbf{w}^* &= \arg \min_{\mathbf{w} \in \mathbb{R}^p} WIS_\alpha(\mathbf{y}) + r \cdot Pen(\mathbf{w}), \quad Pen(\mathbf{w}) = \sum_{i=1}^p (w_i - \bar{w})^2 \\ \text{s.t.} \quad & \bar{w} = \frac{1}{p} \sum_{i=1}^p w_i \end{aligned} \quad (3)$$

4.2 Optimization

Underneath the hood, `postforecasts` accesses the `optim()` function from the `stats`⁷ package. Out of the available optimization methods, BFGS (Fletcher 2013) and L-BFGS-B (Byrd et al. 1995) turned out to be the most reliable for QSA.

⁷<https://www.rdocumentation.org/packages/stats/versions/3.6.2/topics/optim>

BFGS is named after Broyden, Fletcher, Goldfarb and Shanno and a quasi-Newton method. L-BFGS-B is a limited memory version of BFGS and additionally supports box constraints. As default value we set the optimization method to L-BFGS-B as it converges faster than BFGS in our data set, due to its limited memory property. The time gain is especially important for the `qsa_flexible_symmetric` and `qsa_flexible` methods which take considerably longer than `qsa_uniform` due to the large number of quantiles. Furthermore L-BFGS-B also has the advantage that we can lower bound the quantile spread factor to zero and thereby prevent quantile crossing with the median.

The optimization method can be accessed in the `update_predictions()` function by means of the `optim_method` argument. For L-BFGS-B, the lower and upper bound box constraints can be set with the arguments `lower_bound_optim` and `upper_bound_optim`.

Besides the use of `optim()`, `postforecasts` also provides a line search optimization which is used by setting the `optim_method` to `line_search`. As the run time increases exponentially with the parameter space, this method is currently restricted to the `qsa_uniform` method. It runs QSA for all values of the QSA factor within a sequence. This sequence is defined by its upper and lower values set with the arguments `lower_bound_optim` and `upper_bound_optim` as well as its step size set by `steps_optim`.

Regarding the QSA optimization functions shape, there is a potential issue: Due to the trade-off between sharpness and coverage defining the WIS, it might happen that an interval of QSA factors result in the same score. In other words, the WIS loss function has *plateaus*. This becomes less likely the more observations and quantiles are available, nevertheless it still has to be kept in mind.

The `line_search` optimization handles multiple optima by choosing the value closest to 1, hence the smallest possible adjustment of the quantiles. In essence, this is a regularization. For the BFGS and L-BFGS-B algorithms plateaus mean that both methods can converge to different optima while attaining the same WIS. In a future version of the package we aim to tackle this by adding a line search after the use of BFGS and L-BFGS-B in order to find the optima closest to 1 and thereby regularize the results.

Furthermore, due to the long computation times, particularly for large data sets and small initial training periods, the `postforecasts` package provides the option to run QSA *in parallel*. The parallelization is implemented with the `foreach`⁸ package (Revolution Analytics and Weston, n.d.). It can be activated by defining a parallel processing environment and then specifying `parallel = TRUE` within the `update_predictions()` function. A parallel processing environment is defined by setting the number of cores available with the `registerDoParallel()` function from the `doParallel`⁹ package (Corporation and Weston 2022).

The following commands are valid for a device with two available cores:

```
library(postforecasts)
library(doParallel)
registerDoParallel(cores = 2)

df_updated_parallel <- update_predictions(
  df,
  methods = "qsa_flexible",
  optim_method = "L-BFGS-B",
  lower_bound_optim = 0,
  upper_bound_optim = 5,
  parallel = TRUE,
  verbose = TRUE
)
```

To observe the progress of the computations users can set the `verbose = TRUE` in order to print the logging output that the `foreach()` function provides.

⁸<https://www.rdocumentation.org/packages/foreach/versions/1.5.2>

⁹<https://www.rdocumentation.org/packages/doParallel/versions/1.0.16>

Table 11: QSA Uniform improves WIS by increasing interval widths.

method	interval score	dispersion	underprediction	overprediction
original	65.74	12.00	5.83	47.91
qsa_uniform	60.00	26.84	3.44	29.73
qsa_flexible_symmetric	60.92	33.22	2.49	25.21
qsa_flexible	60.47	25.31	9.31	25.84

4.3 Results

As for the CQR method, we investigate how well QSA performs for post-processing Covid-19 forecasts. We focus on the UK Covid-19 Forecasting Challenge data set due to computational restrictions.

4.3.1 Aggregate

We begin by examining a high-level overview of the results. Table 11 presents the performance of all three QSA flavors on the validation set, aggregated over all *models*, *target types*, *horizons* and *quantiles*.

Starting with `qsa_uniform`, we observe clear improvements in the WIS as it drops by -8.73%. As expected, this first update increases the overall dispersion and hence the weighted prediction intervals by a factor of 2.24. The wider intervals therefore cover more observations which reduces the under- and overprediction by -40.98% and -37.95%.

Interestingly, while both decreases are similar in relative terms, their *absolute* effects differ substantially. The underprediction reduction decreases the WIS by -2.39 which amounts to a relative WIS decrease of merely -3.63 %, while the overprediction drops by -18.18 which is equal to a WIS drop by -27.66 %.

We can thus conclude that the main driver behind the increase of the intervals is their *overcoverage*. In other words: the intervals do not reach low enough. Overall, by increasing the intervals and achieving better coverage of smaller observations, while at the same time sacrificing interval sharpness, `qsa_uniform` improves the WIS.

Due to the restriction of identical quantile spread adjustments for all quantiles, the optimization cannot differ in its post-processing of the various intervals. We speculate that smaller intervals might need different adjustments than larger ones. This can be the case if humans have difficulty of intuitively grasping the concept of confidence intervals, especially since we have seen that the adjustments of `qsa_uniform` are quite substantial. This line of reasoning is our motivation behind the `qsa_flexible_symmetric` method. It allows the QSA adjustments to vary between intervals. Its only restriction is that the updates with regards to the lower and upper bounds must be *symmetric*.

Table 11 also presents the aggregated performance of `qsa_flexible_symmetric`. It reports that the WIS remains lower in comparison to the original data, however it lies above the value of `qsa_uniform` by -7.33%. In the aggregate `qsa_flexible_symmetric` seems to overfit compared to the much more restrictive `qsa_uniform`. Further evidence of overfitting is that the dispersion continues to increase with a factor of 2.77 and that the underprediction as well as overprediction drop even lower by -3.33% and -22.7%.

`qsa_uniform` and `qsa_flexible_symmetric` are both restricted to symmetrically adjust upper and lower bounds of the prediction intervals. This is sensible for adjusting models producing residuals that follow a symmetric distribution. If, in contrast, model residuals are *skewed*, and thus the interval coverage lacks more heavily on one side, symmetric adjustments lead to sub-optimal results.

This happens because the model is confronted with a trade-off where it adjusts one side too little and the other side too much. If, for example, QSA wants to *increase* intervals to reduce underprediction or overprediction, it will do so until the gains in coverage are equal to the dispersion penalty for an additional increase in interval width. For a symmetric adjustment, on unsymmetrical data, it will find an adjustment below the optimum for the one end with a lack of coverage, because due to the symmetry, it increases dispersion two

Table 12: QSA Methods differ in performance across Models.

model	method	wis	dis	under	over
EuroCOVIDhub-baseline	uniform	1.41	151.79	-38.53	-33.79
EuroCOVIDhub-baseline	symmetric	2.26	240.03	-60.99	-53.30
EuroCOVIDhub-baseline	flexible	41.41	151.80	-85.95	116.68
EuroCOVIDhub-ensemble	uniform	-2.33	50.93	-26.07	-18.72
EuroCOVIDhub-ensemble	symmetric	-1.03	86.75	-35.61	-29.04
EuroCOVIDhub-ensemble	flexible	0.49	51.77	26.47	-26.16
epiforecasts-EpiExpert	uniform	-10.91	110.29	-49.31	-36.45
epiforecasts-EpiExpert	symmetric	-10.33	150.09	-67.84	-43.74
epiforecasts-EpiExpert	flexible	-10.12	119.72	118.81	-47.80
epiforecasts-EpiExpert_Rt	uniform	-8.74	120.80	-48.07	-36.26
epiforecasts-EpiExpert_Rt	symmetric	-7.59	184.67	-62.42	-48.76
epiforecasts-EpiExpert_Rt	flexible	-18.07	91.64	153.22	-60.41
epiforecasts-EpiExpert_direct	uniform	-10.43	122.49	-47.78	-38.19
epiforecasts-EpiExpert_direct	symmetric	-9.78	154.27	-50.21	-44.34
epiforecasts-EpiExpert_direct	flexible	-12.15	124.66	145.45	-50.99
seabbs	uniform	-12.91	199.50	-56.50	-49.32
seabbs	symmetric	-9.98	273.52	-77.04	-58.13
seabbs	flexible	-15.62	153.56	338.63	-63.88

fold, as the interval is also widens on the other end and this adjustment leads to a dispersion penalty larger than the coverage benefit. The issue is analogous if QSA *decreases* intervals. Thus, if the model residuals are non-symmetric, symmetric methods lead to sub-optimal adjustments on both sides of the interval.

As the Covid-19 infection and death data is inherently non-symmetrically distributed since the observation values are naturally contained in the interval between $[0, \infty)$ and result from exponential growth, we expect model residuals to be skewed towards higher values. Therefore, we examine how the non-symmetric post-processing method `qsa_flexible` adjusts the forecasts and how it preforms in contrast to `qsa_uniform` and `qsa_flexible_symmetric`.

Table 11 presents the aggregated performance of `qsa_flexible` on the validation set. The WIS is a clear improvement in comparison to the original data and lies between `qsa_uniform` and `qsa_flexible_symmetric`. Thus, it performs slightly better than the `qsa_uniform` and slightly worse than the `qsa_flexible_symmetric` methods. Our main interest, however, lies in how intervals are adjusted, i.e. in the dispersion, underprediction and overprediction.

The dispersion increases after post-processing, yet to a lesser degree than for the other methods. The underprediction, most notably and in contrast to the symmetric approaches, substantially increases by 59.76%, while still remaining the lowest of the three WIS components. The overprediction behaves similarly to the `qsa_flexible_symmetric` method and decreases strongly by -46.06%.

Due to the asymmetric nature of the miscoverage, `qsa_flexible` moves the intervals downwards in the aggregate by heavily decreasing the lower quantiles in order to reduce overprediction and slightly decreasing the upper quantiles as the lost coverage is more than compensated by a reduction in dispersion. Due to the nature of exponential growth we would have expected human forecasters to *underestimate* trends. However, for the UK Data, we observe an overconfidence that cases and the death toll will continue to rise.

In the following subsections we increase the granularity of our analysis and examine the QSA flavor performances across the dimensions of our data, namely the *models*, *target types*, *horizons* and *quantiles*.

4.3.2 Models

Table 12 displays the results of QSA post-processing for all three methods stratified by model. These more granular results reveal a pattern that is not visible in the aggregated results: The `qsa_flexible` method performs significantly worse for the EuroCOVIDhub-baseline model by increasing the WIS by 41.41%. It overfits the training set as indicated by Figure 16.

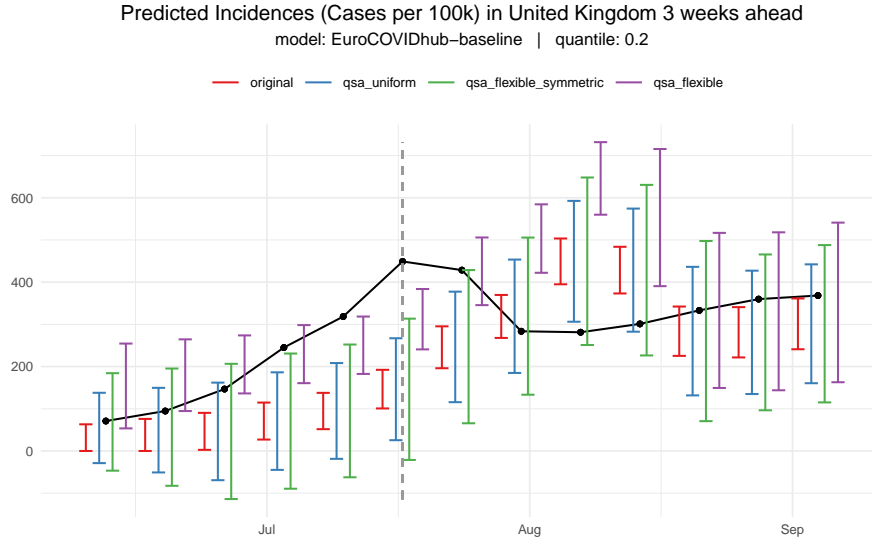


Figure 16: QSA Flexible overfits as its intervals are too low in the training and too high in the validation set.

The figure shows that the original prediction intervals are below the actual values in the training period, then adjust to *overshoot* the actual values and level out during the validation period. As `qsa_flexible` is able to adjust the intervals in a non-symmetrical manner, it learns to push both interval bounds upwards during the training set. As this pattern of underprediction changes in the validation set and the QSA metrics equally weigh all observations, `qsa_flexible` takes some observations to adjust properly and overpredicts the observations in the meantime. In contrast, `qsa_uniform` and `qsa_flexible_symmetric` overfit much less due to their constraint of symmetric adjustments, yet they similarly do *not* improve the WIS in the validation set.

For the EuroCOVIDhub-ensemble model we observe that the `qsa_uniform` method has the best performance and reduces the WIS by -2.33. It seems that a simple, quite restrictive uniform adjustment across all quantile levels provides the largest benefit. Adding additional flexibility among intervals with `qsa_flexible_symmetric` actually *reduces* the gains by about half and the further flexibility of `qsa_flexible` with non-symmetric adjustments even leads to a slightly worse prediction. These results are quite encouraging as the EuroCOVIDhub-ensemble model represents an ensemble of modeling approaches by professional forecasting models and is therefore not burdened by human overconfidence.

For the human forecasting models, namely `epiforecasts-EpiExpert`, `epiforecasts-EpiExpert_Rt`, `epiforecasts-EpiExpert_direct` and `seabbs`, we observe that all QSA methods significantly improve the WIS. Furthermore, for each model there is at least one method that can reduce the score by over 10%.

Regarding the last three models we even see a similar pattern among post processing method performances: `qsa_flexible` reduces the WIS most, followed by `qsa_uniform` and `qsa_flexible_symmetric`. For the first method this ranking is reversed, although the scores vary only slightly. An inspection of the WIS components provides further insight: `qsa_flexible` consistently reduces overprediction the most, is the only method that increases underprediction and has the lowest increase in dispersion. These observations are the result of the non-symmetric adjustments which allow `qsa_flexible` to reduce the lower bound without having to increase the upper counterpart. For the optimization this has two effects: First, it can decrease the lower bound much stronger since the cost in terms of dispersion is cut in half. Second, it can now freely adjust the

Table 13: Across both Target Types all QSA methods improve the WIS.

target type	qsa_uniform	qsa_flexible_symmetric	qsa_flexible
Cases	-0.09	-0.07	-0.08
Deaths	-0.09	-0.10	-0.06

upper quantile until the increase in underprediction is balanced out with the reduction in dispersion.

4.3.3 Target Types

Comparing the QSA methods across target types reveals notable differences. Table 13 shows the relative changes in WIS after applying `qsa_uniform`, `qsa_flexible_symmetric` and `qsa_flexible` to the original data broken down by `target_type`. In the aggregate all three methods improve the score for both target types within a similar range. `qsa_flexible_symmetric` performs best for Covid-19 Deaths and `qsa_uniform` for Cases.

If we split the forecasting models into human and non-human groups the results change as is shown by Figure 17. Human forecasts primarily benefit from post processing Covid-19 **Cases**, while model forecasts are only improved in their Deaths predictions.

As discussed for the human forecast models `qsa_flexible` reduces the WIS most followed by `qsa_uniform` and `qsa_flexible_symmetric`. In terms of overfitting, we observe that `qsa_flexible` is the model that increases the score most. These results illustrate once again that `qsa_flexible` is a riskier model, as it can lead to higher gains or losses due to its potential to fit the training data too closely.

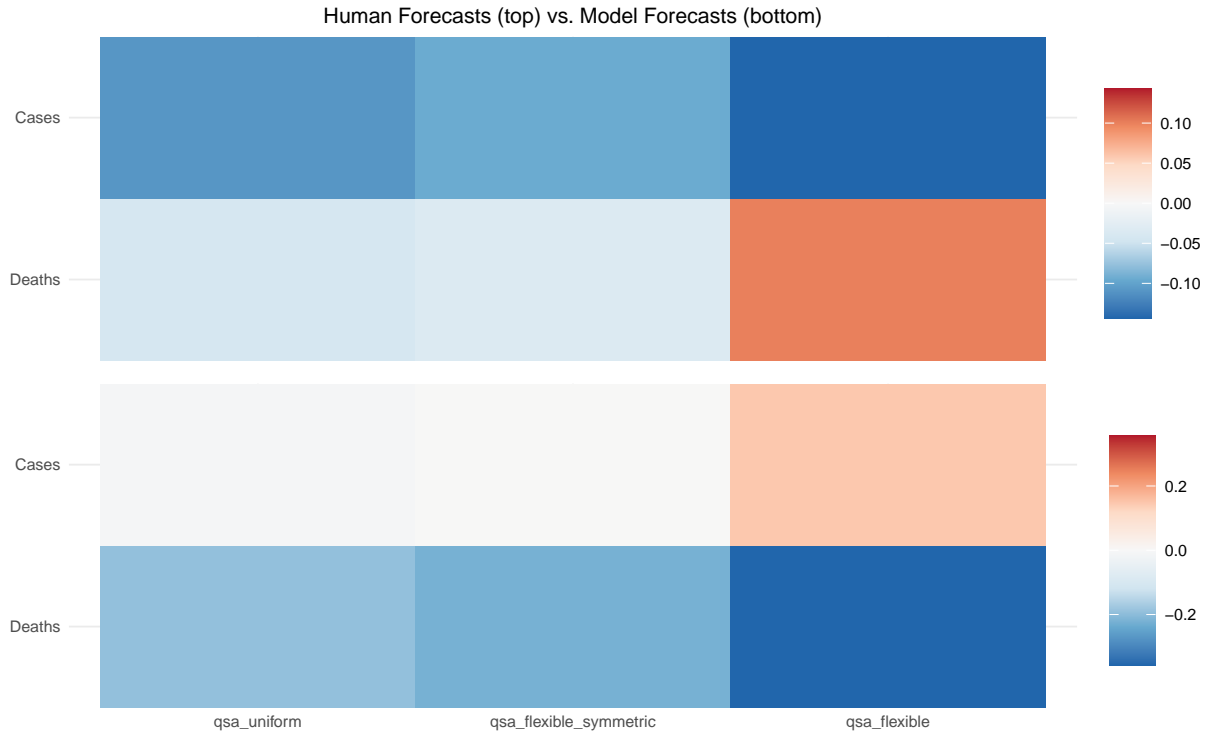


Figure 17: Forecasting improvements differ across target types for different model groups. Human forecasts are primarily improved for Covid-19 Cases, while model forecast improvements are only found for Covid-19 Deaths.

4.3.4 Horizons

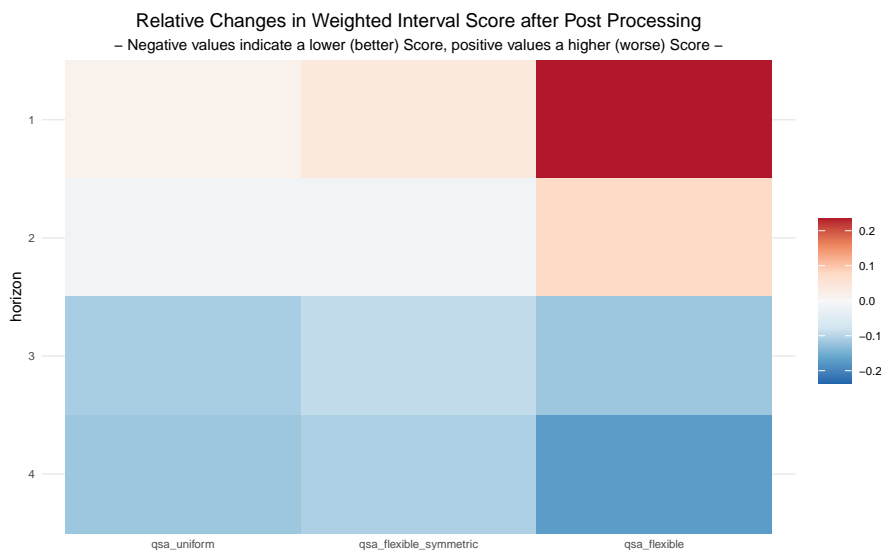


Figure 18: QSA methods improve forecasts more for larger horizons. For smaller horizons they tend to overfit, this is especially the case with QSA Flexible.

Breaking down the results by the forecasting **horizon** also reveals notable patterns. Figure 18 plots the WIS changes across horizons for all three methods. Across all QSA methods the improvements of the WIS increase with the **horizon** level. The gains are primarily visible for the three and four week-ahead predictions. In contrast, the increases in score and overfitting are primarily located at a horizon of one.

Again, a split of the post processed models into human and model forecasts reveals differences as shown by Figure 19. We observe that the aggregate gains solely stem from the human forecasts and that the losses in the WIS are primarily from the model forecasts. Here the method performances also vary more: The largest gains and losses are reported for **qsa_flexible**, while **qsa_uniform** and **qsa_flexible_symmetric** also indicate improvements but overfit much less.

Additionally, breaking down the results by target types reveals the patterns in Figure 26 and Figure 27 in the Appendix. They show gains for death and losses for case predictions across the board for model forecasts. Again, these tendencies are strongest for the **qsa_flexible** flavor of QSA. Human predictions are primarily improved for Covid-19 Cases and forecast horizons of 3 and 4 weeks. For Covid-19 Deaths **qsa_flexible** worsens the score for shorter horizons in particular, while **qsa_uniform** and **qsa_flexible_symmetric** slightly improve the scores across all horizons.

Overall there is a tendency that forecast improvements increase and the risk of overfitting simultaneously drops with increasing forecast horizons.

4.3.5 Quantiles

WIS improvements also vary across different quantile levels. As shown in Figure 20 the improvements are larger for more extreme quantiles. For smaller prediction intervals between the 0.25 and 0.75 quantiles almost no improvements can be observed for any of the three flavors.

This finding is particularly important regarding **qsa_flexible_symmetric**, as the main motivation behind it was to allow for individual adjustments of each interval pair. Thus, we would have expected **qsa_flexible_symmetric** to perform better, particularly for intervals which **qsa_uniform** could not improve due to its restrictive nature. Apparently, the intervals with coverage equal or smaller than 50% were already quite optimal in the original human forecasts.

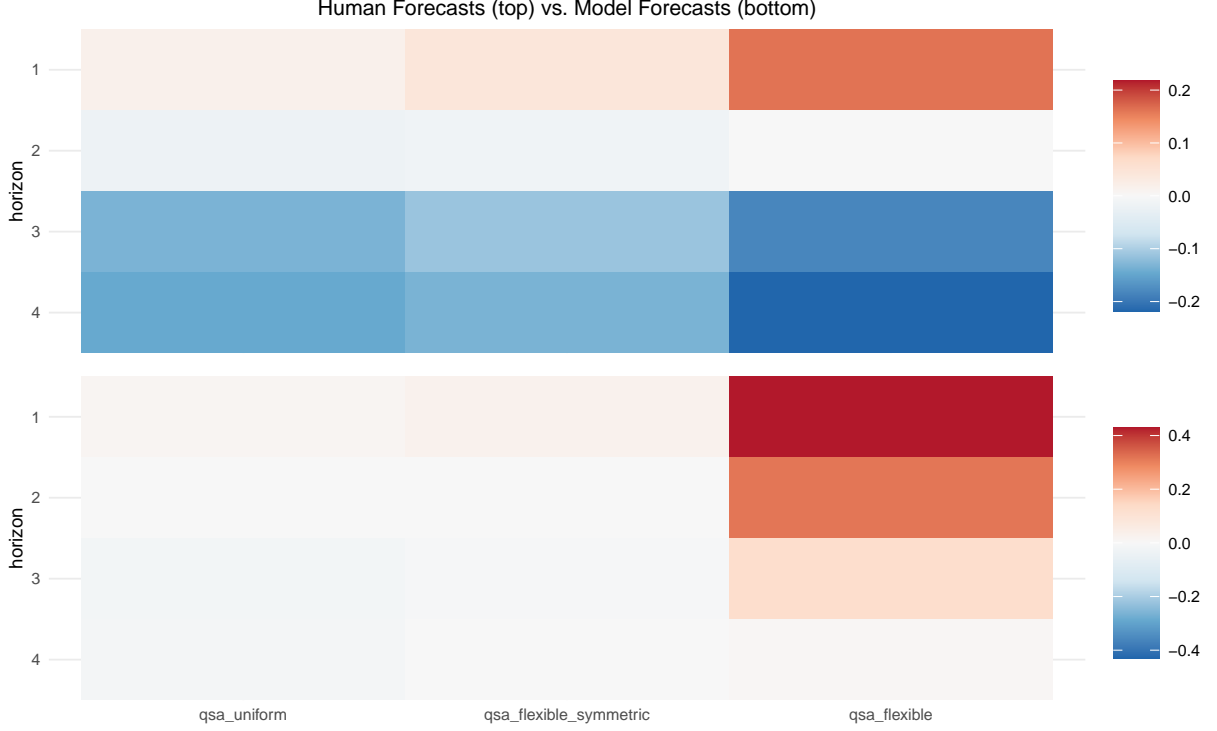


Figure 19: Forecasting improvements differ across horizons for different model groups. Human forecasts are primarily improved for horizons larger than 2, while model forecast are not improved at all and are overfitted with QSA Flexible.

Furthermore, the gains for the larger intervals remain similar, which suggests that the restriction to adjust all intervals with the same quantile spread factor, did not pose an issue for the UK data set.

Yet, aggregation across the `target_type` and `model` dimensions do not represent the full picture, such that we also show the quantile improvements for the human forecasts of Cases as well as the model forecasts of Deaths in Figure 21. For human forecasts of Covid-19 Cases the patterns remain similar to the aggregate. For model forecasts of Covid-19 Deaths, however, we observe larger improvements and detect that `qsa_flexible` is useful for small intervals. This suggests that Death prediction intervals benefit from non-symmetric adjustments. Furthermore, model forecasts of Deaths also seem to be one of the rare situations where `qsa_flexible_symmetric` outperforms `qsa_uniform`.

Subsetting the above results to a forecast horizon of three and four weeks reveals an exception to the look of the quantile graphs. For large forecast horizons and model forecasts of Deaths, we observe worse WIS after the adjustments. These stem from the high cost of not covering an observation at extreme quantiles. Figure 22 exemplifies this where all QSA methods substantially reduce the interval sizes in order to decrease dispersion, which then results in undercoverage of the last week of August.

Thus, the QSA adjustments can underestimate uncertainty at extreme quantiles, especially for short time series as the 13 weeks of the UK data. This risk increases with the flexibility of the QSA flavor.

4.3.6 Conclusion

Overall `qsa_uniform` is the QSA flavor that performs best for the UK data set. It produces notable improvements to the WIS in the validation set without overfitting the training data. The additional flexibility among interval adjustments that `qsa_flexible_symmetric` provides does not lead to significant gains.

Most surprisingly, `qsa_uniform` can not improve the WIS for smaller prediction intervals. It rather has the tendency to slightly overfit the data. The additional flexibility of non-symmetric interval adjustments offered

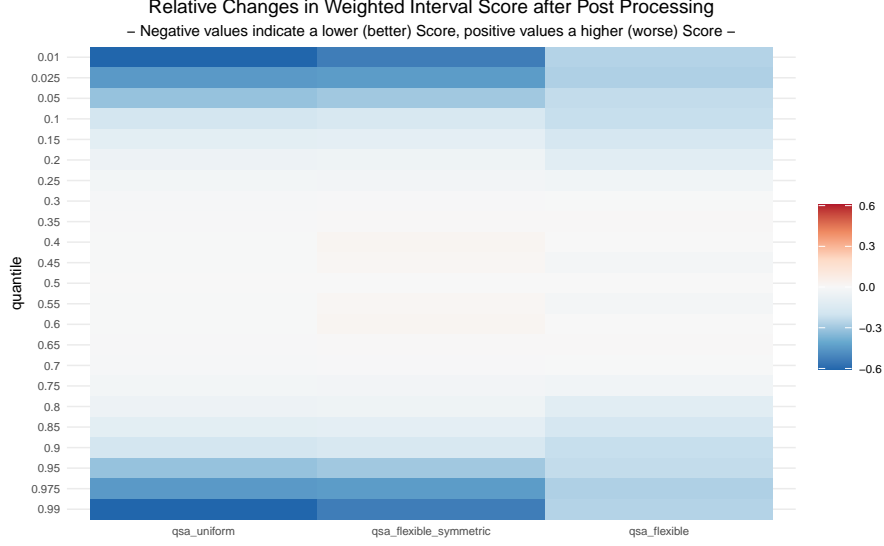


Figure 20: QSA improves forecasters more for more extreme quantiles and thus larger intervals.

by `qsa_flexible` have less clear effects. Overall, `qsa_flexible` and `qsa_flexible_symmetric` can not lower the WIS more than `qsa_uniform`, yet `qsa_flexible` outperforms the other methods in the scenarios where post processing is most useful. `qsa_flexible` substantially overfits the data due to its non-symmetric adjustments as became evident for the EuroCOVIDhub-baseline model.

In general `qsa_uniform` is the more conservative choice, while `qsa_flexible` can be a better fit for data requiring large and varying adjustments across quantiles. With regards to the question when to use QSA, it performs best when forecasts underestimate uncertainty which was the case for larger horizons as well as more extreme quantiles. Furthermore, the method performance also depends on the types of forecasting models as well as the target type. Both taken separately, QSA worked best for human forecast models and Covid-19 Case predictions.

Observed together we did find that QSA performed best for the human forecasts of Cases and model forecasts of Deaths. The former observations are in line with the hypothesis that humans can not grasp uncertainty as well as models and that forecasting uncertainty is higher for Covid-19 Cases than for Deaths, since Deaths are strongly linked to *past* Cases.

Finally, these results leave much room for further investigations and improvements to the QSA method. First, it would be interesting to see whether the described results generalize to the European Forecast Hub data set. This would be particularly interesting as it contains longer time series and hence the models have more data to learn from, which could be an advantage for the more flexible methods. Second, a natural step would be to apply `qsa_flexible_symmetric` and `qsa_flexible` with *penalization*. This option requires keeping some observations in a separate test set as we would fit the penalty value to the validation set.

In regards to additional methods, one could imagine an asymmetric version of `qsa_uniform` with one adjustment for the quantiles below and one for those above the median. With this method one could investigate whether gains observed with `qsa_flexible` can be attributed solely to the asymmetry or are rather to the flexibility across interval levels.

In general, it would be desirable to allow users to set custom restrictions to the vector of QSA factors. Regarding penalization, it might also be interesting to add a penalization form that penalizes towards no adjustments, i.e. pulling all QSA factors closer to a value of one. Moreover, one could weigh the importance of observations in the optimization by their time point. Therefore we suggest an *exponential smoothing* approach that could assign larger weights to more recent observations which would allow the optimization of QSA to adapt faster to changes in the data. This modification would introduce a smoothing hyperparameter that, similar to the penalty approach, requires an additional learning step on the validation set.

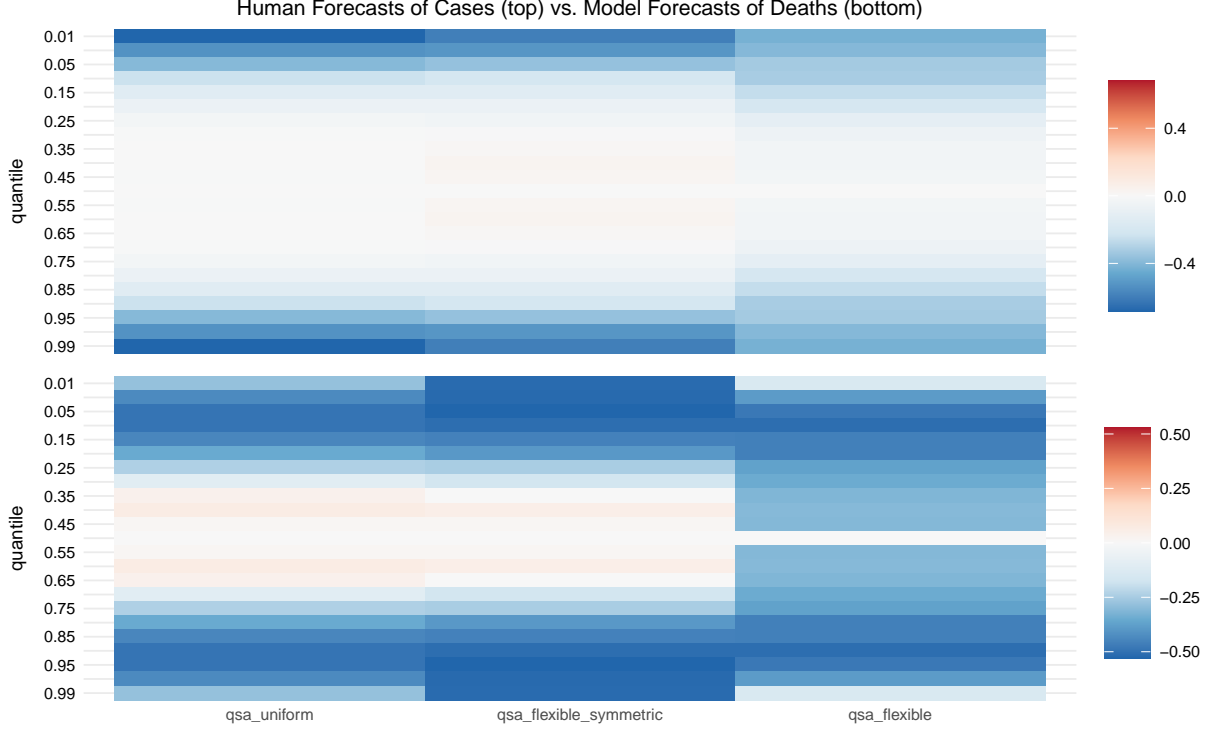


Figure 21: QSA Flexible overfits as its intervals are too low in the training and too high in the validation set.

5 Method Comparison

This chapter aims to compare the effectiveness of all post-processing methods that were introduced throughout previous chapters. In particular, we investigate if some methods consistently *outperform* other procedures across a wide range of scenarios. Further, it will be interesting to observe the *types* of adjustments to the original forecasts: Some methods might improve the Weighted Interval Score by *extending* the interval width and thus increasing coverage, whereas others might yield a comparable final score by *shrinking* the prediction intervals leading to higher precision. One can imagine even more variations: Moving the interval bounds farther apart or closer together can happen *symmetricly* or *asymmetricly* and the interval's midpoint might stay *fixed* or get *shifted* by the post-processing algorithm.

Before jumping into the analysis, we propose one additional model that, in contrast to those we have covered so far, does not add any new information to the equation. Instead, it *combines* the predictions from existing post-processing methods to build an *ensemble* prediction. The idea is that leveraging information from multiple independent algorithms can stabilize estimation since the ensemble learns to focus on the strongest individual model within each area of the feature space. Next, we explain the mathematical reasoning behind the ensemble model in more detail.

5.1 Ensemble Model

There exist various options how to generally combine multiple building blocks into one ensemble. We chose an approach that can be efficiently computed by well-understood optimization algorithms and, at the same time, is highly interpretable. Each quantile prediction of our ensemble model is a *convex combination* of the individual methods, i.e. a linear combination where all weights are contained in the unit interval and sum up to one. Hence, the resulting value lives on the same scale as the original predictions and each weight can be interpreted as the *fractional contribution* of the corresponding building block method.

Consider one particular feature combination of `model`, `location`, `horizon`, `target_type` and `quantile`. Let n specify the number of observations in the training set within this combination, $\mathbf{y} \in \mathbb{R}^n$ the vector of true

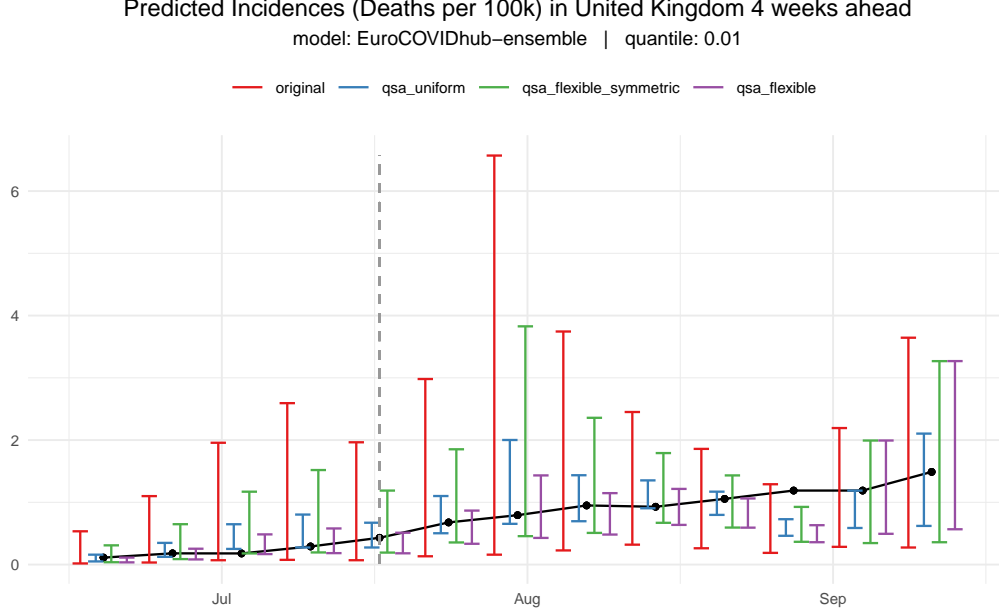


Figure 22: QSA can underestimate uncertainty for extreme quantiles and few data points to learn from.

values, $\mathbf{l}_1, \dots, \mathbf{l}_k \in \mathbb{R}^n$ vectors of original lower quantile predictions and $\mathbf{u}_1, \dots, \mathbf{u}_k \in \mathbb{R}^n$ vectors of original upper quantile predictions from k different post-processing procedures.

Then, for each such combination, the ensemble model computes weights $\mathbf{w}^* \in [0, 1]^k$ by solving the following nonlinear constrained optimization problem:

$$\begin{aligned} \mathbf{w}^* &= \arg \min_{\mathbf{w} \in [0, 1]^k} IS_\alpha(\mathbf{y}) = \arg \min_{\mathbf{w} \in [0, 1]^k} (\mathbf{u} - \mathbf{l}) + \frac{2}{\alpha} \cdot (\mathbf{l} - \mathbf{y}) \cdot \mathbb{1}(\mathbf{y} \leq \mathbf{l}) + \frac{2}{\alpha} \cdot (\mathbf{y} - \mathbf{u}) \cdot \mathbb{1}(\mathbf{y} \geq \mathbf{u}), \\ \text{with } \quad \mathbf{l} &= \sum_{j=1}^k w_j \mathbf{l}_j, \quad \mathbf{u} = \sum_{j=1}^k w_j \mathbf{u}_j \\ \text{s.t.} \quad &\|\mathbf{w}\|_1 = \sum_{j=1}^k w_j = 1, \end{aligned}$$

where all operations for vector inputs \mathbf{l} , \mathbf{u} and \mathbf{y} are understood elementwise and the *same* weights w_j , $j = 1, \dots, k$ are chosen for lower and upper quantiles.

Hence, we choose the (nonlinear) Interval Score (Section 2.1.3) as our objective function that we minimize subject to linear constraints. The optimization step is implemented with the `nloptr`¹⁰ package (Ypma and Johnson 2022), which describes itself as “an R interface to NLOpt, a free/open-source library for nonlinear optimization”.

Note that, technically, the weight vector has to be denoted by $\mathbf{w}_{m,l,h,t,q}^*$ since the computed weights are generally different for each feature combination. We omit the subscripts at this point to keep the notation clean.

The Interval Score always considers *pairs* of quantiles α and $1 - \alpha$ as outer bounds of a $(1 - 2\alpha) \cdot 100\%$ prediction interval. The best results are achieved when a separate weight vector for each quantile pair is computed. Since our data sets contain 11 quantile pairs, 2 target types, 4 horizons and we consider 6 different forecasting models, the ensemble model requires solving $11 \cdot 2 \cdot 4 \cdot 6 = 528$ nonlinear optimization problems for each location, which amounts to $18 \cdot 528 = 9504$ optimization problems for the European Hub Data Set.

¹⁰<https://cran.r-project.org/web/packages/nloptr/index.html>

Due to this high computational cost the *maximum number of iterations* within each optimization is an important hyperparameter that balances the trade-off between computational feasibility and sufficient convergence of the iterative optimization algorithm. Here, we ultimately settled with 10,000 maximum steps which could ensure convergence with respect to a *tolerance level* of 10^{-8} in the vast majority of cases.

Finally, it is worth noting that the weight vector of the ensemble model \mathbf{w}^* is learned on a *training set* such that a fair comparison with all individual post-processing methods on a separate *validation set* is possible.

5.2 Comparison of CQR, QSA & Ensemble

Now that we have introduced *Conformalized Quantile Regression* in Section 3, *Quantile Spread Averaging* in Section 4 and the *Ensemble* Model in Section 5.1, the obvious question is which of the methods performs best. This section conducts a detailed comparison across various feature combinations. Due to the high computational demands of Quantile Spread Averaging, we limit the discussion to the compact UK Covid-19 Forecasting Challenge data set. The results that constitute the starting point of the analysis can be generated with the following commands:

```
library(postforecasts)

df_updated <- uk_data |>
  update_predictions(
    methods = c(
      "cqr", "cqr_asymmetric", "qsa_uniform", "qsa_flexible", "qsa_flexible_symmetric"
    ),
    cv_init_training = 0.5
  ) |>
  collect_predictions() |>
  add_ensemble()
```

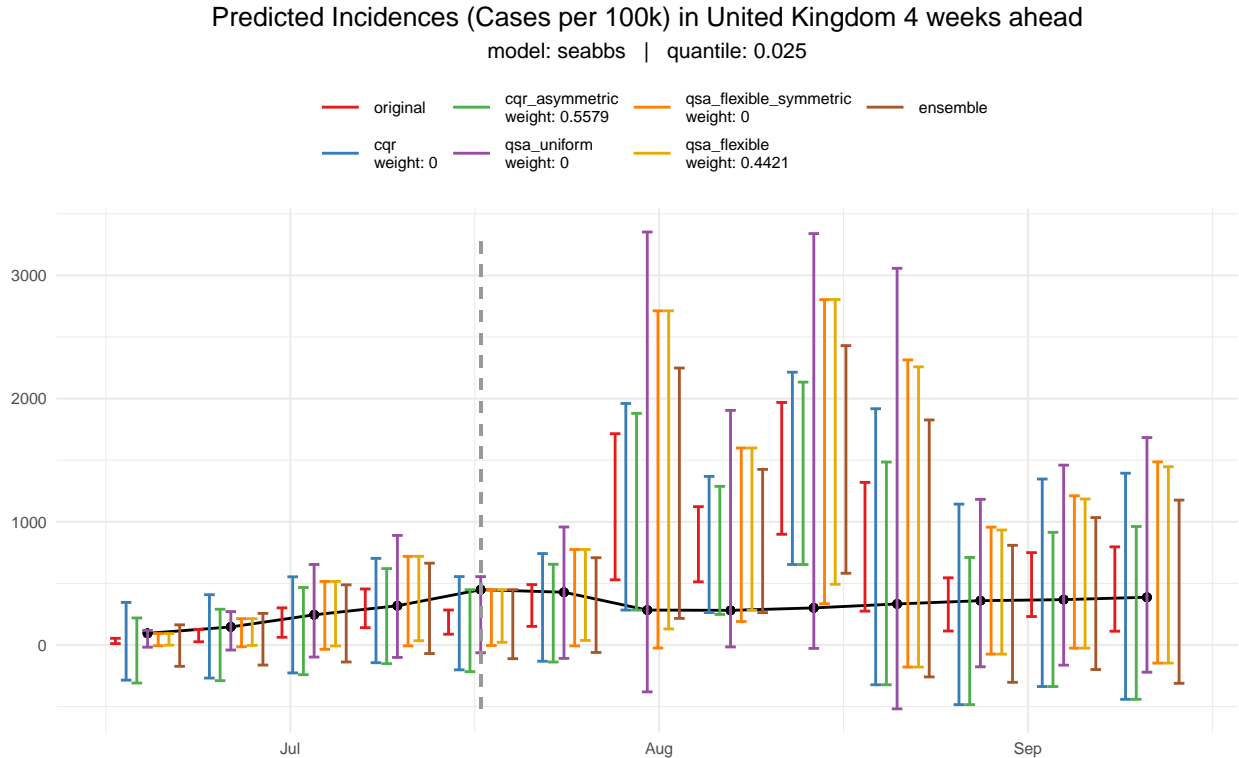


Figure 23: Comparison of Prediction Intervals for all Post-Processing Methods including the Ensemble

Table 14: WIS of all Post-Processing Methods on Training and Validation Set on UK Data

method	validation score	training score	dispersion
ensemble	57.69	18.22	21.73
qsa_uniform	60.00	20.88	26.84
qsa_flexible	60.47	19.48	25.31
qsa_flexible_symmetric	60.92	20.49	33.22
cqr	62.15	20.82	24.10
cqr_asymmetric	63.97	14.46	17.99
original	65.74	23.62	12.00

Figure 23 provides a visual illustration of original and adjusted prediction intervals of all post-processing methods including the ensemble. It is important to note that the relative differences between all methods highly depend on the selected feature combination. For demonstration purposes we chose the `seabbs` model in combination with a large forecast horizon and a small quantile. As we have seen on multiple occasions throughout the previous chapters, this configuration correlates with large adjustments to the original forecasts. For a random example of the feature space the effect sizes and the effect differences between the methods would likely be much smaller such that Figure 23 is not representative but still useful in order to gain some basic intuition.

Except for the last observations on the horizontal axis the forecasts of the two CQR versions are quite similar and significantly closer to the original predictions than the QSA intervals. Within the QSA family `qsa_flexible` and `qsa_flexible_symmetric` produce almost identical corrections whereas `qsa_uniform` behaves quite differently from all other methods and consistently causes the largest intervals. The side-by-side comparison nicely illustrates that the traditional CQR version is the only method which adjusts lower and upper bounds symmetrically by an equal amount. Since the ensemble method is a linear combination of the individual methods, its corrections are generally not symmetric and the produced intervals are usually centered around a different midpoint than the original forecasts.

Figure 23 corresponds to exactly one combination of `model`, `target_type`, `horizon` and `quantile` (pair). Thus, there exists exactly one optimization problem and one set of ensemble weights for this situation. The weights are identical for lower and upper bounds and across all time steps. The color legend displays the ensemble weights: In this case only the asymmetric CQR and the flexible (not symmetric) QSA methods contribute to the ensemble. As a simple weighted average with weights close to 0.5 the lower (upper) bounds of the ensemble intervals are approximately halfway between the lower (upper) bounds of the `cqr_asymmetric` and `qsa_flexible` intervals.

Figure 23 shows that different methods can have significantly different effects, yet it does not provide any hints which method improves the Weighted Interval Score most. Table 14 collects the WIS for each method on the training and validation set, aggregated over all models, target types, horizons and quantiles and sorted by increasing validation score. There are a couple of interesting findings:

- All six custom methods improve out-of-sample performance compared to the original predictions on the UK data set.
- All three QSA versions lead to lower validation scores than any CQR variant. Thus, based on this first impression, the family of QSA post-processing methods clearly outperforms the CQR algorithm for the UK data.
- The ensemble model is the clear winner: Combining information from multiple QSA and CQR methods works better on new data than any individual method on its own. This suggests that the five building block methods are not redundant in the sense that they have different strengths and weaknesses depending on the location in feature space.
- The asymmetric CQR method suffers most from *overfitting*. Compared to the European Forecast

Table 15: Fraction of Feature Combinations where largest Ensemble Weight exceeds Threshold

> 0.5	> 0.9	> 0.99
0.97	0.73	0.55

Table 16: Number (Row 1) and Fraction (Row 2) of largest Ensemble Weights for each Method

cqr	cqr_asymmetric	qsa_uniform	qsa_flexible_symmetric	qsa_flexible
12.00	225.00	1	25.00	265.0
0.02	0.43	0	0.05	0.5

Hub data, where overfitting was not a major issue as described in Section 3.2, the more flexible CQR modification results in the lowest training but highest validation score for the small UK data set.

- In general, additional design restrictions such as identical weights in case of **qsa_uniform** and/or the symmetry assumption in case of **cqr** and **qsa_flexible_symmetric** have some kind of *regularization* effect which leads to better generalization to the validation set. Indeed, the *least* flexible versions of both method frameworks indicate the best validation performance and yet, unsurprisingly, the worst training score.
- All methods improve the original forecasts by *expanding* the prediction intervals which is indicated by the larger *dispersion* values. **qsa_flexible_symmetric** produces by far the widest intervals on average, yet we can not observe a correlation of better validation scores and either narrower or wider prediction intervals.

Table 14 convincingly demonstrates that the ensemble model leads to the best forecasts. Thus, we want to gain more insight how the ensemble predictions are created in this specific use case. Recall that the weights for each of the five building block methods are by construction nonnegative and (in case of convergence) sum to one. A different set of weights is computed for each of the $6 \cdot 2 \cdot 4 \cdot 11 = 528$ combinations of **model**, **target_type**, **horizon** and **quantile** (pairs). One question of interest is if the optimization algorithm tends more towards evenly distributed weights within each combination by assigning a positive weight to many component methods, or rather selects a single winning method (or two as in Figure 23) with a weight of 1 and all remaining methods are discarded with a weight of 0.

Table 15 provides a first insight into the weight distribution of the ensemble model. In 97% of all feature combinations a single method has a larger weight than all of the competing methods combined. Further, in more than half of the optimization solutions the ensemble emulates one particular method by concentrating the entire weight mass on a single point. Hence, although we can not observe a strict *winner takes it all* procedure, the weight distribution is heavily skewed towards one contributing component at each location in feature space.

Now that we have discovered that there seems to be a single method that clearly outperforms its competition for most covariate combinations, we want to find out *which* of the five post-processing methods takes the winning trophy most often. Table 16 displays the frequency with which the ensemble assigns the largest weight to each method. The first row contains the absolute number of times and the second row the fraction of all 528 optimization problems where the methods contributed most to the ensemble model.

In more than 90% of cases the largest weight is given to either the asymmetric CQR or the flexible QSA method whereas the uniform QSA method almost never has the largest impact on the ensemble. This finding is particularly interesting in comparison with Table 14: Since the ensemble is fitted on the *training* set, it distributes the weights according to the training set performance of each individual method. **cqr_asymmetric** and **qsa_flexible** indeed have the best training scores whereas **qsa_uniform** performs worst on the training set which exactly corresponds to the order of Table 16. With this connection in mind it seems even

more surprising that the ensemble method generalizes very well to out-of-sample data while simultaneously rewarding potentially overfitting methods like `cqr_asymmetric` during its own learning process.

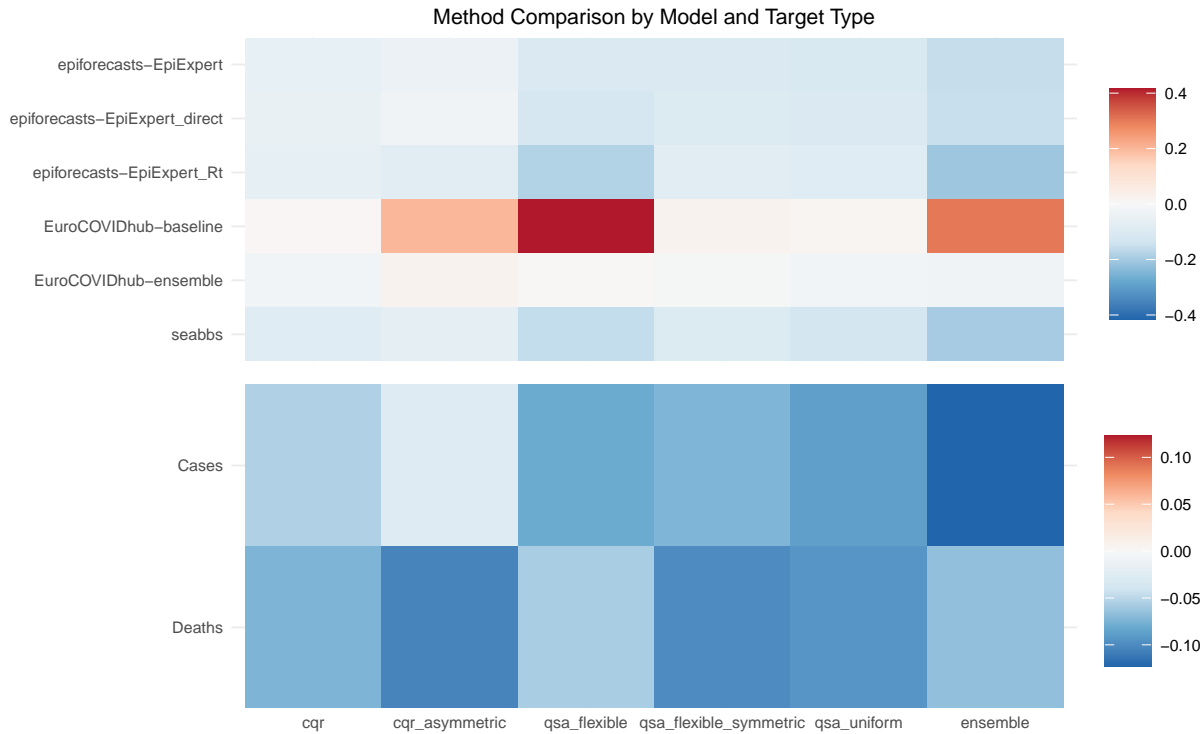


Figure 24: Method Comparison for each Forecasting Model and Target Type

Finally, we compare the different methods within each of the four major categories. Figure 24 shows relative improvements stratified either by forecasting model (top) or by target type (bottom). The picture is surprisingly diverse: Discriminating between the models first the `epiforecasts-EpiExpert_Rt` and the `seabbs` model benefit most overall whereas the `EuroCOVIDhub-baseline` model shows a negative effect for `cqr_symmetric` and `qsa_flexible`. In confirmation of Table 16 the latter two are exactly the methods with the strongest impact on the ensemble which, indeed, cannot improve the original forecasts for the `EuroCOVIDhub-baseline` model either. For all other models the flexible non-symmetric QSA version and the ensemble consistently outperform the remaining alternatives.

The ambiguity of the results is even more highlighted by the bottom plot. Based on the heatmap alone we cannot draw any conclusions if Cases or Deaths benefit more from post-processing in general, the effects simply vary too much across different methods. Comparing within the columns `qsa_flexible` and the ensemble are the only methods which indicate stronger benefits for Covid-19 Cases, all alternatives perform better for Deaths. Within the rows Figure 24 reveals the ensemble model as a good post-processing choice for Covid Cases, while `cqr_asymmetric` and `qsa_flexible_symmetric` show promising results for Covid Deaths.

When stratifying by forecast horizons and quantiles in Figure 25, the similarities between the methods are much stronger than in Figure 24. As we already know from previous chapters, all methods generally work better for larger horizons and quantiles in the tails. As usual the ensemble predictions are closest to `qsa_flexible` and lead to the largest performance gains for three and four week-ahead predictions while simultaneously indicating the *worst* results for short-term one week ahead forecasts. The classical `cqr` method is the only method that reliably works for any forecast horizon, yet the effect sizes are quite small.

The bottom plot of Figure 25 provides a deeper understanding on the interaction between post-processing method and quantile level. `qsa_flexible_symmetric` and `qsa_uniform` have the largest positive effect for very small or very large quantiles with a significant drop in performance towards the center. In contrast, the

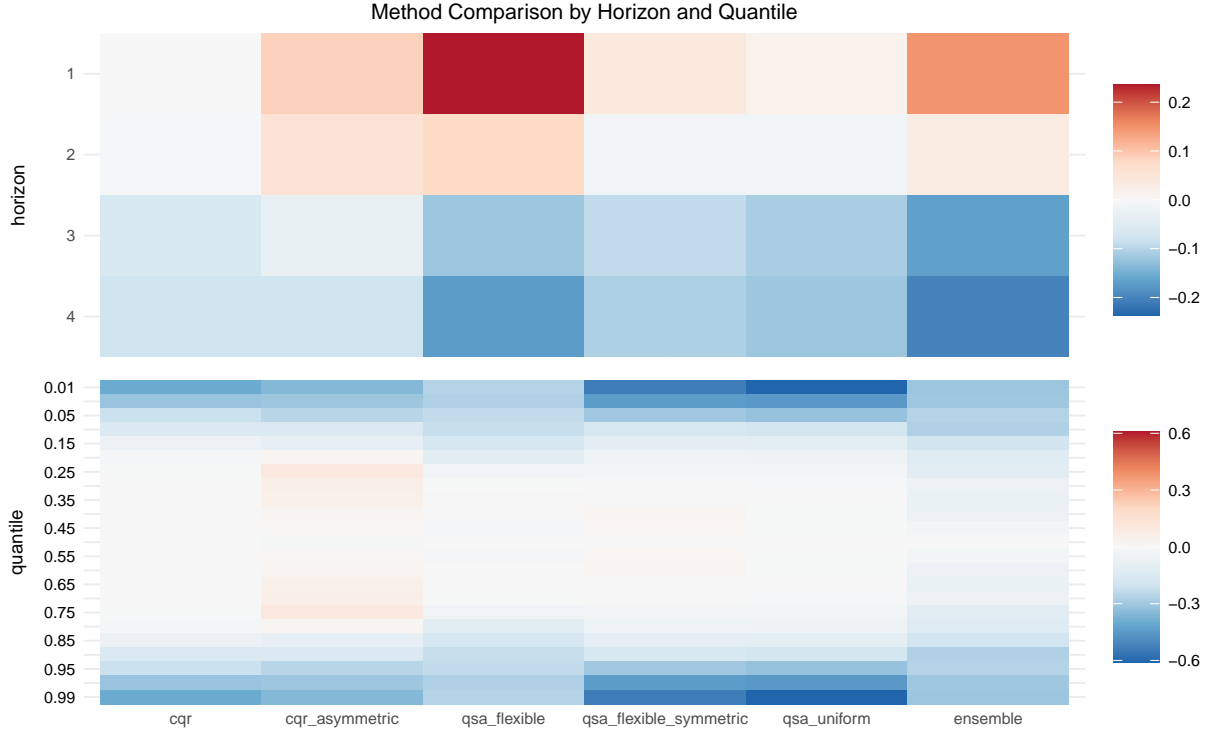


Figure 25: Method Comparison for each Forecast Horizon and Quantile Level

`qsa_flexible` and the ensemble method cause more balanced improvements that are less sensitive to the location of the predictive distribution. The asymmetric CQR version is the only method with a (partially) negative impact and should thus be avoided for post-processing forecasts of centered quantiles.

In summary, Figure 24 and Figure 25 do not allow generic recommendations which post-processing method should be used. The ensemble model as the overall winner from Table 14 tends to have the largest effect sizes, both in positive and negative direction (except for the quantile plot). It thus offers a good choice if upsides and downsides contribute equally to the user’s cost function. In case of risk aversion the traditional CQR method might be preferable, it is the only method which *exclusively* leads to performance improvements for all category levels across both figures.

6 Conclusion

This project investigated the effects of post-processing Covid-19 forecasts.

We focused on two families of post-processing algorithms, Conformalized Quantile Regression and Quantile Spread Averaging, and explained key characteristics of each method. Starting from the original CQR and the simplest uniform QSA method, we revealed their theoretical limitations and linked them to empirical findings in real-world data sets. Further, we proposed two modifications within each family which lead to greater flexibility and could potentially solve the detected shortcomings.

Finally, we compared the out-of-sample performance of each method. For the UK Covid-19 Forecasting Challenge data QSA improved the original forecasts by a greater amount than CQR. The best overall performance, however, is achieved by combining information of the individual methods into one ensemble model. Throughout the comparison we gained a deeper understanding by analyzing similarities and differences within and between the two post-processing frameworks CQR and QSA and showed that there is not a single method that dominates its competition across the entire feature space. Rather, the performance ranking highly depends on the original forecasting model, the forecast horizon, the quantile level and, in the context

of Covid-19 predictions, the target type, i.e. Covid-19 Cases or Covid-19 Deaths.

From a technical perspective, we developed a fully functional R package which implements all individual post-processing methods and the ensemble model. The package is designed to be easily extendable in the future with few changes to the user interface. Due to computational hurdles that we faced during the implementation of Quantile Spread Averaging we leveraged parallel computing to make computations feasible.

There exist multiple directions to extend our work. The most straightforward approach is to research and implement further post-processing algorithms and compare their effectiveness with the existing methods. Further, one could apply our methods to more general forecasting domains unrelated to Covid-19 predictions and analyze which methods generalize best to new contexts. From a more global perspective, it might be valuable to collaborate with research groups of similar interests and integrate our package into a generic time series forecasting framework that unites the entire process of data pre-processing, constructing prediction models and ultimately fine tuning prediction results via post-processing.

Beyond our own project, we believe that research with respect to developing and understanding post-processing of time series forecasts is far from saturated and there remain many opportunities to consolidate and broaden the current state of knowledge.

A QSA Appendix

QSA across Horizons and Target Types for different Models

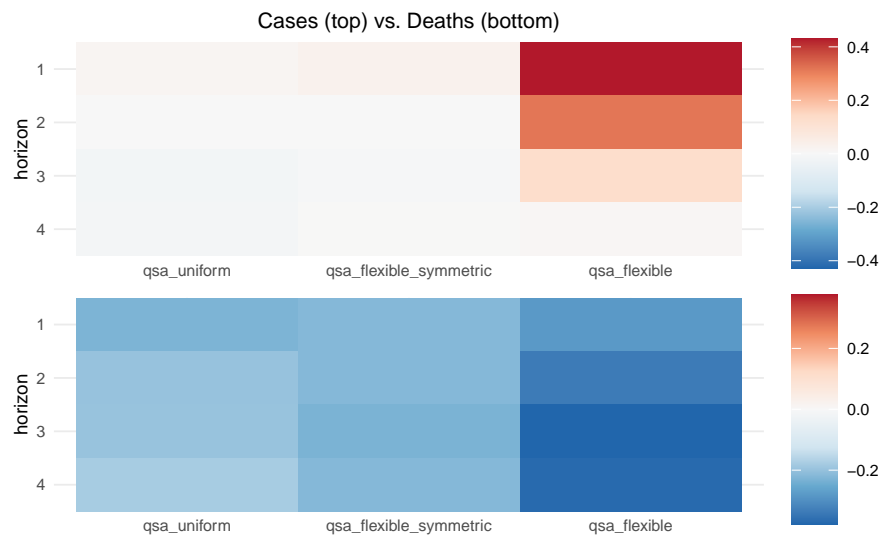


Figure 26: Forecasting improvements differ across horizons and target types for model forecasts. Model forecasts only improved across all horizons for the death predictions

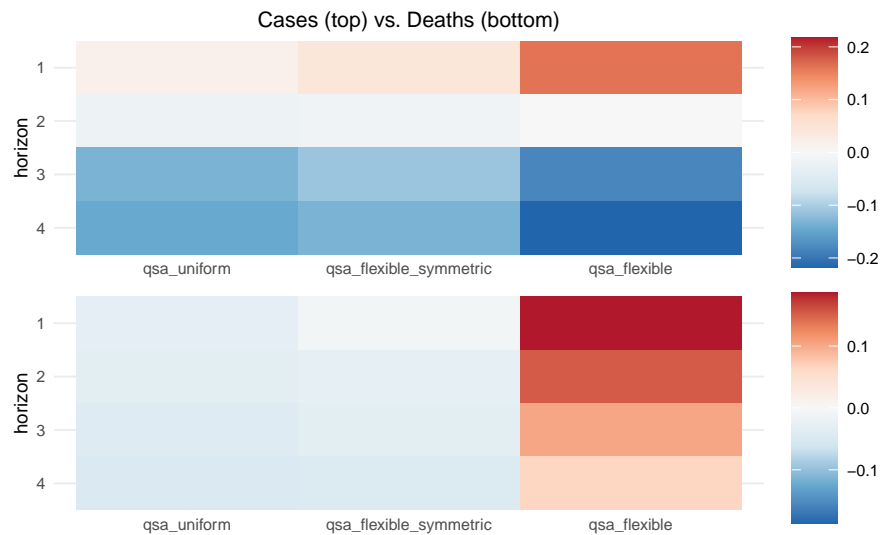


Figure 27: Forecasting improvements differ across horizons and target types for model forecasts. Human forecasts are primarily improved for cases and the horizons of 3 and 4 weeks ahead. For deaths `qsa_flexible` worsens the score

References

- Bassett, Gilbert, and Roger Koenker. 1982. “An Empirical Quantile Function for Linear Models with | Operatornameiid Errors.” *Journal of the American Statistical Association* 77 (378): 407. <https://doi.org/10.2307/2287261>.
- Bosse, Nikos, Sam Abbott, and Hugo Gruson. 2022. *Scoringutils: Utilities for Scoring and Assessing Predictions*.
- Bracher, Johannes, Evan L. Ray, Tilmann Gneiting, and Nicholas G. Reich. 2021. “Evaluating Epidemic Forecasts in an Interval Format.” *PLOS Computational Biology* 17 (2): e1008618. <https://doi.org/10.1371/journal.pcbi.1008618>.
- Byrd, Richard H, Peihuang Lu, Jorge Nocedal, and Ciyu Zhu. 1995. “A Limited Memory Algorithm for Bound Constrained Optimization.” *SIAM Journal on Scientific Computing* 16 (5): 1190–1208.
- Corporation, Microsoft, and Steve Weston. 2022. *doParallel: Foreach Parallel Adaptor for the Parallel Package*. <https://github.com/RevolutionAnalytics/doparallel>.
- EpiForecasts. 2021a. “European Covid-19 Forecast Hub.” London School of Hygiene and Tropical Medicine, European Centre for Disease Control and Prevention (ECDC). <https://covid19forecasthub.eu/index.html>.
- . 2021b. “UK Covid-19 Crowd Forecasting Challenge.” London School of Hygiene & Tropical Medicine, European Centre for Disease Control and Prevention (ECDC). <https://www.crowdforecastr.org/2021/05/11/uk-challenge/>.
- Fletcher, Roger. 2013. *Practical Methods of Optimization*. John Wiley & Sons.
- Gnanvi, Janyce Eunice, Kolawolé Valère Salako, Gaëtan Brezesky Kotanmi, and Romain Glèlè Kakaï. 2021. “On the reliability of predictions on Covid-19 dynamics: A systematic and critical review of modelling techniques.” *Infectious Disease Modelling* 6: 258–72. <https://doi.org/10.1016/j.idm.2020.12.008>.
- Gneiting, Tilmann, and Adrian E Raftery. 2007. “Strictly Proper Scoring Rules, Prediction, and Estimation.” *Journal of the American Statistical Association* 102 (477): 359–78. <https://doi.org/10.1198/016214506000001437>.
- Hyndman, Rob, and George Athanasopoulos. 2021. *Forecasting: Principles and Practice*. Third. OTexts. <https://otexts.com/fpp3/>.
- R Core Team. 2021. *R: A Language and Environment for Statistical Computing*. Vienna, Austria: R Foundation for Statistical Computing. <https://www.R-project.org/>.
- Revolution Analytics, and Steve Weston. n.d. *Foreach: Provides Foreach Looping Construct*.
- Romano, Yaniv, Evan Patterson, and Emmanuel J. Candès. 2019. “Conformalized Quantile Regression.” *arXiv:1905.03222 [Stat]*, May. <http://arxiv.org/abs/1905.03222>.
- Tibshirani, Ryan. 2019. “Advances and Challenges in Conformal Inference.” Carnegie Mellon University. <https://www.stat.cmu.edu/~ryantibs/talks/conformal-2019.pdf>.
- Ypma, Jelmer, and Steven G. Johnson. 2022. *Nloptr: R Interface to NLOpt*. <https://CRAN.R-project.org/package=nloptr>.